The Habitability of Proxima Centauri b I: Evolutionary Scenarios

Rory Barnes[1,2,3], Russell Deitrick[1,2], Rodrigo Luger[1,2], Peter E. Driscoll[4,2], Thomas R. Quinn[1,2], David P. Fleming[1,2], Benjamin Guyer[1,2], Diego V. McDonald[1,2], Victoria S. Meadows[1,2], Giada Arney[1,2], David Crisp[5,2], Shawn D. Domagal-Goldman[6,2], Andrew Lincowski[1,2], Jacob Lustig-Yaeger[1,2], Eddie Schwieterman[1,2]

ABSTRACT

We analyze the evolution of the potentially habitable planet Proxima Centauri b to identify environmental factors that affect its long-term habitability. We consider physical processes acting on size scales ranging between the galactic scale, the scale of the stellar system, and the scale of the planet's core. We find that there is a significant probability that Proxima Centauri has had encounters with its companion stars, Alpha Centauri A and B, that are close enough to destabilize Proxima Centauri's planetary system. If the system has an additional planet, as suggested by the discovery data, then it may perturb planet b's eccentricity and inclination, possibly driving those parameters to non-zero values, even in the presence of strong tidal damping. We also model the internal evolution of the planet, evaluating the roles of different radiogenic abundances and tidal heating and find that a planet with chondritic abundance may not generate a magnetic field, but all other models do maintain a magnetic field. We find that if planet b formed *in situ*, then it experienced ∼160 million years in a runaway greenhouse as the star contracted during its formation. This early phase may have permanently desiccated the planet and/or produced a large abiotic oxygen atmosphere. On the other hand, if Proxima Centauri b formed with a thin hydrogen atmosphere ($\lesssim$ 1% of the planet's mass), then this envelope could have

[1]Astronomy Department, University of Washington, Box 951580, Seattle, WA 98195

[2]NASA Astrobiology Institute – Virtual Planetary Laboratory Lead Team, USA

[3]E-mail: rory@astro.washington.edu

[4]Department of Terrestrial Magnetism, Carnegie Institution for Science, Washington, DC

[5]Jet Propulsion Laboratory, California Institute of Technology, M/S 183-501, 4800 Oak Grove Drive, Pasadena, CA 91109

[6]Planetary Environments Laboratory, NASA Goddard Space Flight Center, 8800 Greenbelt Road, Greenbelt, MD 20771

shielded the water long enough for it to be retained before being blown off itself. Through modeling a wide range of Proxima b's evolutionary processes we identify pathways for planet b to be habitable and conclude that water retention is the biggest obstacle for planet b's habitability. These results are all obtained with a new software package called VPLANET.

1. Introduction

The discovery of Proxima Centauri b, hereafter Proxima b, heralds a new era in the exploration of exoplanets. Although very little is currently known about it and its environment, the planet is likely terrestrial and receives an incident flux that places it in the "habitable zone" (HZ) (Kasting et al. 1993; Selsis et al. 2007; Kopparapu et al. 2013). Moreover, Proxima b is distinct from other discoveries in that it is the first potentially habitable planet that could be directly characterized by space telescopes such as WFIRST, concept missions such as LUVOIR, HDST, and HabEx, and/or planned 30-meter class ground-based telescopes. Proxima b could be the first exoplanet to be spectroscopically probed for active biology.

The interpretation of these spectra require a firm understanding of the history of Proxima b and its host system. Proxima b exists in an environment that is significantly different from Earth and has likely experienced different phenomena that could preclude or promote the development of life. When viewed across interstellar distances, biology is best understood as a planetary process: life is a global phenomenon that alters geochemical and photochemical processes. Spectroscopic indicators of life, *i.e.* biosignatures, can only be identified if the abiotic processes on a planet are understood – no single feature in a spectrum is a "smoking gun" for life. A robust detection of extraterrestrial life requires that all plausible non-biological sources for an observed spectral feature can be ruled out. This requirement is a tall order in light of the expected diversity of terrestrial exoplanets in the galaxy and the plethora of mechanisms capable of mimicking biosignatures (Schwieterman et al. 2016; Meadows et al., in prep.). With these challenges in mind, Proxima b may offer the best opportunity to begin the scientific process of searching for unambiguous signs of life.

In this study, we leverage the known (but sparse) data on Proxima b and its host system to predict the range of evolutionary pathways that the planet may have experienced. As we show below, many evolutionary histories are possible and depend on factors ranging from the cooling rate of b's core to the orbital evolution of the stellar system through the Milky Way galaxy, and everything in between. The evolution of Proxima b, and by extension its potential habitability, depends on physical processes that tend to be studied by scientists

from different fields, such as geophysics and astrophysics. However, for the purpose of interpreting Proxima b, we must overcome these divisions. A critical examination of the potential habitability of Proxima b necessitates a cohesive model that can fold in the impact of the many factors that shape evolutionary history. Our examination of Proxima b will draw on simple, but realistic, models that have been developed in the fields of geophysics, planetary science, atmospheric science and astrophysics. From this synthesis, we identify numerous opportunities and obstacles for life to develop on Proxima b, as well as lay a foundation for the future interpretation of spectroscopic observations.

This paper is organized as follows. In § 2 we review the observational data on the system and the immediate implications for habitability. In § 3 we describe models to simulate the evolution of the system, with a focus on habitability. In this section we introduce a new software package, VPLANET, which couples physical models of planetary interiors, atmospheres, spins and orbits, stellar evolution, and galactic effects. In § 4 we present results of these models. An exhaustive analysis of all histories is too large to present here, so in this section we present highlights and end-member cases that bracket the plausible ranges, highlighting some of the issues Proxima b faces with respect to its habitability. In § 5 we discuss the results and identify additional observations that could improve modeling efforts and connect our results to the companion paper (Meadows et al., in prep.). Finally, in § 6 we draw our conclusions.

2. Observational Constraints

In this section we review what is known about the triple star system Alpha Centauri (hereafter α Cen) of which Proxima Centauri may be a third member. This star system has been studied carefully for centuries as it is the closest to the Sun. We will first review the direct observational data, then we will make whatever inferences are possible from those data, and finally we qualitatively consider how these data constrain the possibility for life to exist on Proxima b, which will then guide the models described in the next section.

2.1. Properties of the Proxima Planetary System

Very little data exist for Proxima b. The radial velocity data reveal a planet with a minimum mass m of 1.27 $M_{\oplus}$, an orbital period P of 11.186 days, and an orbital eccentricity e less than 0.35; Anglada-Escudé (2016) report a mean longitude λ of 110°. These data are the extent of the direct observational data on the planet, but even the minimum mass relies

on uncertain estimates of the mass of the host star, described below.

Proxima b may not be the only planet orbiting Proxima Centauri. The Doppler data suggest the presence of another planetary mass companion with an orbital period near 215 days, but it is not definitive yet (Anglada-Escudé 2016). If present, the second planet has a projected mass of $\lesssim$ 10 $M_\oplus$, consistent with previous non-detections (Endl & Kürster 2008; Barnes et al. 2014; Lurie et al. 2014). The orbital eccentricity and its relative inclination to Proxima b's orbit are also unknown, but as described below, could take any value that permits dynamical stability. Additionally, lower mass and/or more distant planetary companions could also be present in the system.

2.2. Properties of the Host Star

As Proxima Centauri is the closest star to the Sun, it has been studied extensively since its discovery 100 years ago (Innes 1915). It has a radius R_* of 0.14 $R_\odot$, a temperature T_{eff} of 3050 K, a luminosity L_* of 0.00155 $L_\odot$ (Boyajian et al. 2012), and a rotation period P_* of 83 days (Benedict et al. 1998). Anglada-Escudé (2016) find a spectral type of M5.5V. Wood et al. (2001) searched for evidence of stellar winds, but found none, indicating mass loss rates $\dot{M}_*$ less than 20% of our Sun's, *i.e.* < 4 $\times$ 10^{-15} $M_\odot$/yr. Proxima Centauri possesses a much larger magnetic field (B $\sim$ 600 G) than our Sun (B = 1 G) (Reiners & Basri 2008), but somewhat low compared to the majority of low mass stars.

Like our Sun, Proxima Centauri's luminosity varies slowly with time due to starspots (Benedict et al. 1993). HST observations of Proxima Centauri found variations up to 70 milli-magnitudes (mmag) in V (Benedict et al. 1998), which, if indicative of the bolometric luminosity, corresponds to about a 17.5% variation, with a period of 83.5 days (*i.e.* the rotation period). Moreover, Benedict et al. (1998) found evidence for two discrete modes of variability, one lower amplitude mode (ΔV $\sim$ 30 mmag) with a period of $\sim$ 42 days, and a larger amplitude mode (ΔV $\sim$ 60 mmag) with a period of 83 days. These periods are a factor of 2 apart, leading Benedict et al. (1998) to suggest that sometimes a large spot (or cluster of spots) is present on one hemisphere only, while at other times smaller spots exist on opposite hemispheres. Regardless, incident stellar radiation ("instellation") variations of 17% could impact atmospheric evolution and surface conditions of a planet (the sun's variation is of order 0.1% (Willson et al. 1981)).

Additionally, the magnetic field strength may vary with time. Cincunegui et al. (2007) monitored the Ca II H and K lines, which are indicators of chromospheric activity, as well as Hα for 7 years and found modest evidence for a 442 day cycle in stellar activity. Although

the strength of Proxima's magnetic field at the orbit of planet b is uncertain, it could affect the stability of b's atmosphere and potentially affect any putative life on b.

Proxima Centauri is a known flare star (Shapley 1951)[1] and indeed several flares were reported during the Pale Red Dot campaign (Anglada-Escudé 2016). Walker (1981) performed the first study of the frequency of flares as a function of energy, finding that high energy events ($\sim 10^{30}$ erg) occurred about once per day, while lower energy events ($\sim 10^{28}$ erg) occurred about once per hour. Numerous observational campaigns since then have continued to find flaring at about this frequency (Benedict et al. 1998; Anglada-Escudé 2016; Davenport 2016).

2.3. Properties of the Stellar System

Many of the properties of Proxima Centauri are inferred from its relationship to α Cen A and B, thus a discussion of the current knowledge of α Cenis warranted here. Proxima Centauri is $\sim 15,000$ AU from α Cen A and B, but all three have the same motion through the galaxy. The proper motion and radial velocity of the center of mass of α Cen A and B permit the calculation of the system's velocity relative to the sun. Poveda et al. (1996) find the three velocities are $(U, V, W) = $ (-25, -2, 13) km/s for the center of mass. This velocity implies the system is currently moving in the general direction of the Sun, and is on a roughly circular orbit around the galaxy with an eccentricity of 0.07 (Allen & Herrera 1998).

A recent, careful analysis of astrometric and HARPS RV data by Pourbaix & Boffin (2016) found the masses of the two stars to be 1.133 and 0.972 $M_\odot$, respectively, with an orbital eccentricity of 0.52 and a period of 79.91 years. The similarities between both A and B and the Sun, as well as their low apparent magnitudes, has allowed detailed studies of their spectral and photometric properties. These two stars (as well as Proxima) form a foundation in stellar astrophysics, and hence a great deal is known about A and B. However, as we describe below, many uncertainties still remain regarding these two stars.

The spectra of α Cen A and B provide information about the stellar temperature, gravitational acceleration in the photosphere, rotation rate, and chemical composition. That these features can be measured turns out to be critical for our analysis of the evolution of Proxima b. Proxima Centauri is a low mass star with strong molecular absorption lines

---

[1]Although Shapley is the sole author of his 1951 manuscript, the bulk of the work was performed by two assistants, acknowledged only as Mrs. C.D. Boyd, and Mrs. V.M. Nail.

and NLTE effects, which make it extraordinarily difficult to identify elemental abundances; hence its composition is far more difficult to measure than for G and K dwarfs like α Cen A and B (Johnson & Apps 2009). Recently, Hinkel & Kane (2013) completed a reanalysis of published compositional studies, rejecting the studies of Laird (1985) and Neuforge-Verheecke & Magain (1997) because they were too different from the other 5 they considered. Hinkel & Kane (2013) found the mean metallicity [Fe/H] of each of the two stars to be +0.28 and +0.31 and with a large spread of 0.16 and 0.11, respectively. While it is frustrating that different groups have arrived at significantly different iron abundances, it is certain the stars are more metal-rich than the Sun.

Hinkel & Kane (2013) go on to examine 21 other elements, including C, O, Mg, Al, Si, Ca, and Eu. These elements can be important for the bulk composition and/or are tracers of other species that are relevant to planetary processes. In nearly all cases, the relative abundance of these elements to Fe is statistically indistinguishable from the solar ratios. Exceptions are Na, Zn and Eu in α Cen A, and V, Zn, Ba and Nd in α Cen B. The discrepancies between the two stars is somewhat surprising given their likely birth from the same molecular cloud. On the other hand, the high eccentricity of their orbit could point toward a capture during the open cluster phase (*e.g.* Malmberg et al. 2007). For all elements beside Eu, the elemental abundances relative to Fe are larger than in the Sun. In particular, it seems likely that the stars are significantly enriched in Zn.

α Cen A and B are large and bright enough for asteroseismic studies that can reveal physical properties and ages of stars to a few percent, for high enough quality data (Chaplin et al. 2014). Indeed, these two stars are central to the field of asteroseismology, and have been studied in exquisite detail (e.g. Bouchy & Carrier 2001, 2002). However, significant uncertainties persist in our understanding of these stars, despite all the observational advantages.

A recent study undertook a comprehensive Bayesian analysis of α Cen A with priors on radius, composition, and mass derived from interferometric, spectroscopic and astrometric measurements, respectively (Bazot et al. 2016). Their adopted metallicity constraint comes from Neuforge-Verheecke & Magain (1997) via Thoul et al. (2003), which was rejected by the Hinkel & Kane (2013) analysis. They also used an older mass measurement from Pourbaix et al. (2002), which is slightly smaller than the updated mass from Pourbaix & Boffin (2016). They then used an asteroseismic code to determine the physical characteristics of A. Although the mass of A is similar to the Sun at 1.1 $M_{\odot}$, the simulations of Bazot et al. (2016) found that α Cen A's core lies at the radiative/convective boundary and the transition between pp- and CNO-dominated energy production chains in the core. Previous results found the age of α Cen A to be 4.85 Gyr with a convective core (Thévenin et al. 2002), or

6.41 Gyr without a convective core (Thoul et al. 2003). The ambiguity is further increased by uncertainty in the efficiency of the ^{14}N(p,γ)^{15}O reaction rate in the CNO cycle, and by the possibility of convective overshooting of hydrogen into the core. They also consider the role of "microscopic diffusion," the settling of heavy elements over long time intervals. All these uncertainties prevent a precise and accurate measurement of α Cen A's age. Combining the different model predictions and including 1σ uncertainties, the age of α Cen A is likely to be between 3.4 and 5.9 Gyr, with a mean of 4.78 Gyr.

α Cen B has also been studied via asteroseismology, but as with A, the results have not been consistent. Lundkvist et al. (2014) find significant discrepancies between their "Asteroseismology Made Easy" age (1.5 Gyr) with other values, but with uncertainties in excess of 4 Gyr. The asteroseismic oscillations on B are much smaller than on A, which make analyses more difficult (see, *e.g.* , Carrier & Bourban 2003), leading to the large uncertainty. Combining studies of A and B, we must conclude that the ages of the two stars are uncertain by at least 25%. Given the difficulty in measuring B's asteroseismic pulsations, we will rely on A's asteroseismic data and assume the age of A and B to be $4.8^{+1.1}_{-1.4}$ Gyr.

2.4.   Inferences from the Observational Data

Because Proxima b was discovered indirectly, its properties and evolution depend critically on our knowledge of the host star's properties. Although many properties of Proxima Centauri are known, the mass M_{Prox}, age, effective temperature T, and composition are not. The spectra and luminosity suggest the mass of Proxima is $\sim$ 0.12 M$_\odot$ (Delfosse et al. 2000). If we adopt this value, then the semi-major axis of b's orbit is 0.0485 AU and the planet receives 65% of the instellation Earth receives from the Sun (Anglada-Escudé 2016). Note that Sahu et al. (2014) suggested that Proxima's proper motion sent it close enough to two background stars for the general relativistic deflection of their light by Proxima to be detectable with HST and should allow the determination of M_{Prox} to better than 10%, but those results are not yet available.

Additional inferences rely on the assumption that Proxima formed with the α Cen binary. The similarities in the proper motion and parallax between Proxima and α Cen immediately led to speculation as to whether the stars are "physically connected or members of the same drift" (Voûte 1917), *i.e.* are they bound or members of a moving group? The intervening century has failed to resolve this central question. If Proxima is just a random star in the solar neighborhood, Matthews & Gilmore (1993) concluded that the probability that Proxima would appear so close to α Cen is about 1 in a million, suggesting it is very likely the stars are somehow associated with each other. Using updated kinematic information,

Anosova et al. (1994) concluded that Proxima is not bound, but instead part of a moving group consisting of about a dozen stellar systems. Wertheimer & Laughlin (2006)'s reanalysis found that the observational data favor a configuration that is at the boundary between bound and unbound orbits. However, their best fit bound orbit is implausibly large as the semi-major axis is 1.31 pc, *i.e.* larger than the distance from Earth to Proxima. Matvienko & Orlov (2014) also failed to unequivocally resolve the issue, and concluded that RV precision of better than 20 m/s is required to determine if Proxima is bound, which should be available in the data from Anglada-Escudé (2016). Perhaps the discovery data for Proxima b will also resolve this long-standing question.

Regardless of whether Proxima is bound or not, the very low probability that the stars would be so close to each other strongly supports the hypothesis that the stars formed in the same star cluster. We will assume that they are associated and have approximately equal ages and similar compositions. An age near 5 Gyr for Proxima is also consistent with its slow rotation period and relatively modest activity levels and magnetic field (Reiners & Basri 2008).

Planet formation around M dwarfs is still relatively understudied, but it should proceed in a qualitatively similar way as for Sun-like stars, *i.e.* the planet forms from a disk of dust and gas. Relatively few observations of disks of M dwarfs exist (*e.g.* Hernández et al. 2007; Williams & Cieza 2011; Luhman 2012; Downes et al. 2015), but these data seem to point to a wide range of lifetimes for the gaseous disks of 1–15 Myr. This timescale is likely longer than the time to form terrestrial planets in the HZs of late M dwarfs (Raymond et al. 2007; Lissauer 2007), and hence Proxima b may have been fully formed before the disk dispersed. For Proxima, the lifetime of the protoplanetary disk is unknown, and could have been altered by the presence of α Cen A and B, so any formation pathway or evolutionary process permitted within this constraint is plausible.

The radial velocity data combined with M_{Prox} only provide a minimum mass, but significantly larger planet masses are geometrically unlikely, and very large masses can be excluded because they would incite detectable astrometric signals (note that the minimum mass solution predicts an astrometric orbit of the star of ~1 microsecond of arc). It is very likely the planet has a mass less than 10 $M_\oplus$, and probably < 3 $M_\oplus$. We will assume the latter possibility is true, and hence the planet is likely rocky, based on statistical inferences of the population of *Kepler* planets (Weiss & Marcy 2014; Rogers 2015). However, even at the minimum mass, we cannot exclude the possibility that Proxima b possesses a significant hydrogen envelope, and is better described as a "mini-Neptune," which is unlikely to be habitable (but see Pierrehumbert & Gaidos 2011).

If non-gaseous, the composition is still highly uncertain and depends on the unknown

formation process. Several possibilities exist according to recent theoretical studies: 1) the planet formed *in situ* from local material; 2) the planet formed at a larger semi-major axis and migrated in while Proxima still possessed a protoplanetary disk; or 3) an instability in the system occurred that impulsively changed b's orbit. For case 1, the planet may be depleted in volatile material (Raymond et al. 2007; Lissauer 2007), but could still initially possess a significant water reservoir (Ciesla et al. 2015; Mulders et al. 2015). For case 2, the planet would have likely formed beyond the snow line and hence could initially be very water-rich (Carter-Bond et al. 2012). For case 3, the planet could be formed either volatile-rich or poor depending on its initial formation location as well as the details of the instability, such as the frequency of impacts that occurred in its aftermath. We conclude that all options are possible given the data and for simplicity will assume the planet is Earth-like in composition. If we adopt the silicate planet scaling law of Sotin et al. (2007), the radius of a 1.3 $M_\oplus$ planet is 1.07 $R_\oplus$.

2.5.   Implications for Proxima b's Evolution and Habitability

Given the above observations and their immediate implications, this planet may be able to support life. All life on Earth requires three basic ingredients: Water, energy, and the bioessential elements C, H, O, N, S and P. Additionally, these ingredients must be present in an environment that is stable in terms of temperature, pressure and pH for long periods of time. As we describe in this subsection, these ingredients may coexist on Proxima b and hence the planet is potentially habitable, meaning that the planet has long-term persistence of liquid water on the surface.

Proxima's luminosity and effective temperature combined with b's orbital semi-major axis place the planet in the HZ of Proxima and nearly in the same relative position of Earth in the Sun's HZ in terms of instellation. Specifically, the planet receives about 65% of Earth's instellation, which, due to the redder spectrum of Proxima, places b comfortably in the "conservative" HZ of Kopparapu et al. (2013). Even allowing for observational uncertainties, Anglada-Escudé (2016) find that the planet is in this conservative HZ.

However, its habitability depends on many more factors than just the instellation. The planet must form with sufficient water and maintain it over the course of the system age. Additionally, even if water is present, the evolution and potential habitability of Proxima b depends on many other factors involving stellar effects, the planet's internal properties, and the gravitational influence of the other members of the stellar system.

The host star is about 10 times smaller and less massive than the Sun, the temperature is

about half that of the Sun, and the luminosity is just 0.1% that of the Sun. These differences are significant and can have a profound effect on the evolution of Proxima b. Low mass stars can take billions of years to begin fusing hydrogen into helium in their cores, and the star's luminosity can change dramatically during that time. Specifically, the star contracts at roughly constant temperature and so the star's luminosity drops with time. For the case of Proxima, this stage lasted $\sim$ 1 Gyr (Baraffe et al. 2015) and hence Proxima b could have spent significant time interior to the HZ. This "pre-main sequence" (pre-MS) phase could either strip away a primordial hydrogen atmosphere to reveal a "habitable evaporated core" (Luger et al. 2015), or, if b formed as a terrestrial planet with abundant water, it could desiccate that planet during an early runaway greenhouse phase and build up an oxygen-dominated atmosphere (Luger & Barnes 2015). Thus, the large early luminosity of the star could either help or hinder b's habitability.

Low mass stars also show significant activity, *i.e.* flares, coronal mass ejections, and bursts of high energy radiation (*e.g.* West et al. 2008). This activity can change the composition of the atmosphere through photochemistry, or even completely strip the atmosphere away (Raymond et al. 2008). The tight orbit of Proxima b places it at risk of atmospheric stripping by these phenomena. A planetary magnetic field could increase the probability of atmospheric retention by deflecting charged particles, or it could decrease it by funneling high energy particles into the magnetic poles and providing enough energy to drive atmospheric escape. Either way, knowledge of the frequency of flaring and other high energy events, as well as of the likelihood that Proxima b possesses a magnetic field, would be invaluable information in assessing the longevity of Proxima b's atmosphere.

The close-in orbit also introduces the possibility that tidal effects are significant on the planet. Tides can affect the planet in five ways. First, they could cause the rotation rate to evolve to a frequency that is equal to or similar to the orbital frequency, a process typically called tidal locking (Dole 1964; Kasting et al. 1993; Barnes 2016). Second, they can drive the planet's obliquity ψ to zero or 180°, such that the planet has no seasons (Heller et al. 2011). Third, they can cause the orbital eccentricity to change, usually (but not always) driving the orbit toward a circular shape (Darwin 1880; Ferraz-Mello et al. 2008). Fourth, they can cause frictional heating in the interior, known as tidal heating (Peale et al. 1979; Jackson et al. 2008a; Barnes et al. 2013). Finally, they can cause the semi-major axis to decay as orbital energy is transformed into frictional heat, possibly pulling a planet out of the HZ (Darwin 1880; Barnes et al. 2008). Except in extreme cases, these processes are unlikely to sterilize a planet, but they can profoundly affect the planet's evolution (Driscoll & Barnes 2015).

Many researchers have concluded that tidally locked planets of M dwarfs are unlikely

to support life because their atmospheres would freeze out on the dark side (Kasting et al. 1993). However, numerous follow-up calculations have shown that tidal locking is not likely to result in uninhabitable planets (Joshi et al. 1997; Pierrehumbert 2011; Wordsworth et al. 2011; Yang et al. 2013; Shields et al. 2016; Kopparapu et al. 2016). These models all find that winds are able to transport heat to the back side of the planet for atmospheres larger than about 0.3 bars. In fact, synchronous rotation may actually allow habitable planets to exist closer to the host star because cloud coverage develops at the sub-stellar point and increases the planetary albedo (Yang et al. 2013). Thus, tidal locking may increase a planet's potential to support life. However, we note that no study has so far considered a tidally locked planet orbiting a star as cool as Proxima.

Although the abundances of elements relative to iron in α Cen A and B, and by (assumed) extension Proxima, are similar to the Sun's, there is no guarantee that the abundance pattern is matched in Proxima b. Planet formation is often a stochastic process and composition depends on the impact history of a given world. The planet could have formed near its current location, which would have been relatively hot early on and the planet could be relatively depleted in volatiles (Raymond et al. 2007; Mulders et al. 2015). These studies may even overestimate volatile abundances as they ignored the high luminosities that late M dwarfs have during planet formation. Alternatively, the planet could have formed beyond the snow line and migrated in either while the gas disk was still present, or later during a large scale dynamical instability. In those cases, the planet could be volatile-rich.

If the abundances of Proxima are indeed similar to α Cen A and B, then the depletion of Eu in α Cen A is of note as it is often a tracer of radioactive material like ^{232}Th and ^{238}U (Young et al. 2014). These isotopes are primary drivers of the internal energy of Earth, and hence if they are depleted in Proxima b, its internal evolution could be markedly different than Earth's. However, since no depletion is observed in α Cen B, it is far from clear that such a depletion exists. One interesting radiogenic possibility is that the planet could form sufficiently quickly ($\sim$ 1 Myr) that ^{26}Al could still provide energy to the planet's interior. Hence any prediction of b's evolution should also consider its role.

The presence of additional planets can change the orbit and obliquity of planet b through gravitational perturbations. These interactions can change the orbital angular momentum of b and drive oscillations in e, the inclination i, longitude of periastron ϖ, and longitude of ascending node Ω. Changes in inclination can lead to changes in ψ as the planet's rotational axis is likely fixed in inertial space, except for precession caused by the stellar torque, while the orbital plane precesses. These variations can significantly affect climate evolution and possibly even the planet's potential to support life (Armstrong et al. 2014).

If Proxima is bound to α Cen A and B, then perturbations by passing stars and torques

by the galactic tide can cause drifts in Proxima's orbit about A and B (Kaib et al. 2013). During epochs of high eccentricity, Proxima may swoop so close to A and B that their gravity is able disrupt Proxima's planetary system. This could have occurred at any time in Proxima's past and can lead to a total rearrangement of the system. Thus, should additional planets exist in the Proxima planetary system, these could be present on almost any orbit, with large eccentricities and large mutual inclinations relative to b's orbital plane (*e.g.* Barnes et al. 2011).

The inferred metallicity of Proxima Centauri is quite high for the solar neighborhood, which has a mean of -0.11 and standard deviation of 0.18 (Allende Prieto et al. 2004). Indeed, recent simulations of stellar metallicity distributions in the galaxy find that at the sun's galactic radius R_{gal} of ∼8 kpc, stars cannot form with [Fe/H] > +0.15 (Loebman et al. 2016). The discrepancy can be resolved by invoking radial migration (Sellwood & Binney 2002), in which stars on nearly circular orbits are able to ride corotation resonances with spiral arms either inward and outward. Loebman et al. (2016) find that with migration, the metallicity distribution of stars in the Sloan Digital Sky Survey III's Apache Point Observatory Galactic Evolution Experiment (Hayden et al. 2015) is reproduced. Furthermore, Loebman et al. find that stars in the solar neighborhood with [Fe/H] > +0.25 must have formed at $R_{gal} < 4.5$ kpc. Similar conclusions were reached in an analysis of the RAVE survey by Kordopatis et al. (2015). We conclude that this system has migrated outward at least 3.5 kpc, but probably more. As the surface density scale length of the galaxy is ∼2.5 kpc, this implies that the density of stars at their formation radius was at least 5 times higher than at the Sun's current Galactic radius.

The observed and inferred constraints for the evolution of Proxima b are numerous, and the plausible range of evolutionary pathways is diverse. The proximity of two solar-type stars complicates the dynamics, but allows the extension of their properties to Proxima Centauri. In the next sections we apply quantitative models of the processes described in this section to the full stellar system in order to explore the possible histories of Proxima b in detail.

3. Models

In this section we describe the models we use to consider the evolution and potential habitability of Proxima b. We generally use published models that are common to different disciplines of science. Although the models come from disparate sources, we have compiled them all into a new software program called VPLANET. This code is designed to simulate exoplanet evolution, with a focus on habitability. The problem of habitability is interdisciplinary, but we find it convenient to break the problem down into more manageable chunks, which

we call "modules," that are incorporated when applicable. At this time, VPLANET consists of simple models that are all representable as sets of ordinary differential equations. Below we describe qualitatively the modules and direct the reader to the references for a quantitative description. We then briefly describe how VPLANET unifies these modules and integrates the system forward.

3.1. Stellar Evolution: STELLAR

Of the many stellar evolutionary tracks available in the literature (*e.g.* Baraffe et al. 1998; Dotter et al. 2008; Baraffe et al. 2015), we find that the Yonsei-Yale tracks for low-mass stars (Spada et al. 2013) provide the best match to the stellar parameters of Proxima Centauri. We selected the [Fe/H] = +0.3 track with mixing length parameter $\alpha_{\mathrm{MLT}} = 1.0$ and linearly interpolated between the $0.1\,\mathrm{M}_\odot$ and $0.15\,\mathrm{M}_\odot$ tracks to obtain a track at $M_{Prox} = 0.12\,\mathrm{M}_\odot$. While these choices yield a present-day radius within 1σ of $0.1410 \pm 0.0070\,\mathrm{R}_\odot$ (Boyajian et al. 2012), the model predicts a luminosity at $t = 4.78$ Gyr that is $\sim 15\%$ higher than the value reported in Boyajian et al. (2012) (a $\sim 10\sigma$ discrepancy). Such a discrepancy is not unexpected, given both the inaccuracies in the evolutionary models for low mass stars and the large intrinsic scatter of the luminosity and radius of M dwarfs at fixed mass and metallicity, likely due to unmodeled magnetic effects (Spada et al. 2013). Moreover, the large uncertainties in the age, mass, and metallicity of Proxima Centauri (§2) further contribute to the inconsistency.

Nevertheless, since we are concerned with the present-day habitability of Proxima b, it is imperative that our model match the present-day luminosity of its star. We therefore scale the Yonsei-Yale luminosity track down to match the observed value, adjusting the evolution of the effective temperature to be consistent with the radius evolution (which we do not change). We note that this choice results in a *lower* luminosity for Proxima Centauri at all ages, which yields conservative results ("optimistic" in terms of habitability) for the total amount of water lost from the planet (§4.4). Moreover, this adjustment likely has a smaller effect on the qualitative nature of our results than the large uncertainties on the properties of the star and the planet.

We also model the evolution of the XUV luminosity of the star as in Luger & Barnes (2015). We use the power-law of Ribas et al. (2005) with power law exponent $\beta = -1.23$, a saturation fraction $L_{\mathrm{XUV}}/L_{\mathrm{bol}} = 10^{-3}$ and a saturation time of 1 Gyr. These choices yield a good match to the present-day value, $L_{\mathrm{XUV}}/L_{\mathrm{bol}} = 2.83 \times 10^{-4}$ (Boyajian et al. 2012).

In Fig. 1 we plot the stellar model used in this paper, showing the evolution of the
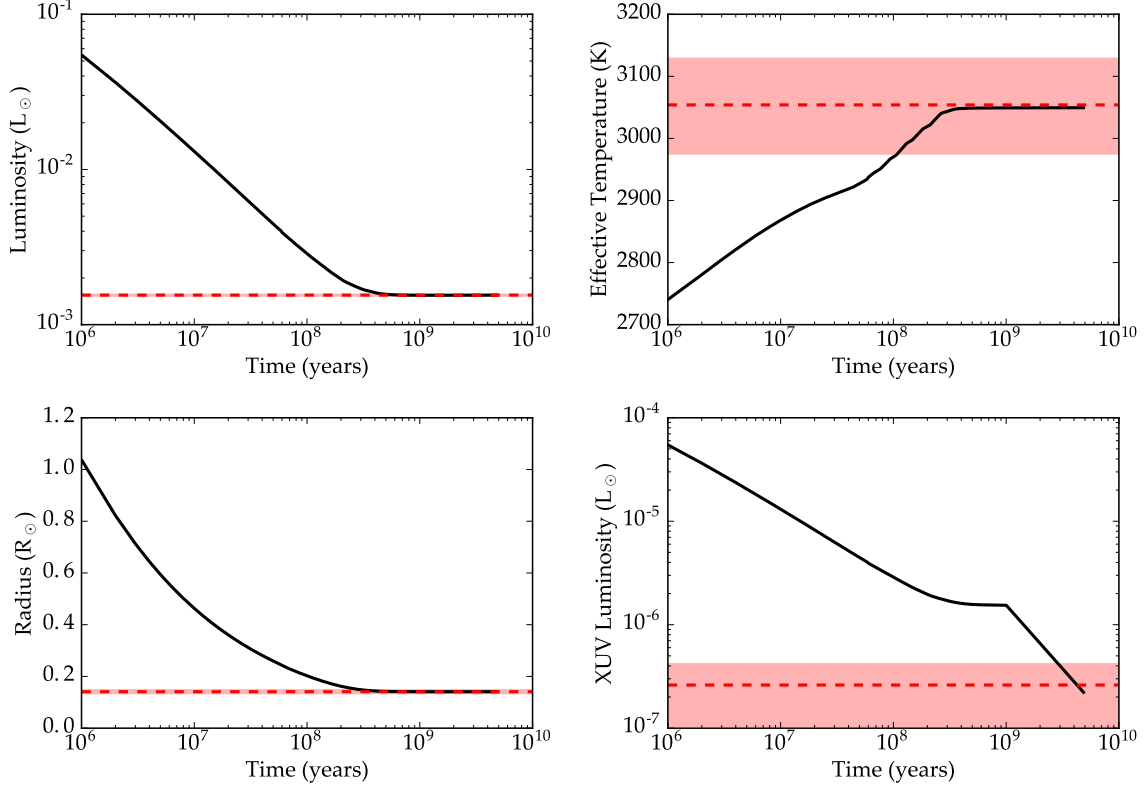
Fig. 1.— Luminosity, temperature, radius, and XUV evolution of Proxima Centauri from $t_0 = 1$ Myr to the present day. The dashed red lines indicate the measured values of each parameter (see text). 1σ uncertainties are shaded in light red. By construction, all tracks match the observed values at the present day within 1σ.

luminosity, radius, effective temperature, and XUV luminosity as a function of time from t_0 = 1 Myr to the mean system age of 4.78 Gyr. The long pre-main sequence (pre-MS) phase studied by Luger & Barnes (2015) is evident, lasting ~ 1 Gyr.

3.2.   Atmospheric Escape: `ATMESC`

We model atmospheric escape under the energy-limited (Watson et al. 1981; Erkaev et al. 2007) and diffusion-limited (Hunten 1973) parameterizations, closely following Luger et al. (2015) and Luger & Barnes (2015). We refer the reader to those papers for a detailed description of the equations and methodology. In this section we outline the main adaptations and improvements to the models therein.

We model both the escape of hydrogen from a putative thin primordial envelope and the escape of hydrogen and oxygen from photolysis of water during an early runaway greenhouse. As in Luger & Barnes (2015), we set water escape rates to zero once the planet enters the HZ, since the establishment of a cold trap should limit the availability of water in the upper atmosphere. We further assume that planets with hydrogen envelopes must lose them completely before water can be lost, given the expected large diffusive separation between light H atoms and heavy H_2O molecules. We shut off hydrodynamic escape at 1 Gyr, the approximate time at which the star reaches the main sequence, to account for the transition to ballistic escape predicted by Owen & Mohanty (2016). We assume XUV escape efficiencies ϵ_{XUV} of 0.15 for hydrogen envelope escape and 0.30 for the escape of a steam atmosphere, whose opacity is larger in the FUV, leading to additional heating (Sekiya et al. 1981). Finally, for hydrogen-rich planets, we use the radius evolution tracks for super-Earths of Lopez et al. (2012) and Lopez & Fortney (2014), enforcing a radius of $1.07\,R_\oplus$ when no hydrogen is present.

The rate of escape of a steam atmosphere closely depends on the fate of photolytically-produced oxygen. We compute the hydrodynamic drag on oxygen atoms using the formalism of Hunten et al. (1987) to obtain oxygen escape rates, tracking the buildup of O_2 in the atmosphere. As in Tian (2015) and Schaefer et al. (2016), we account for the increasing mixing ratio of O_2 at the base of the hydrodynamic flow, which slows the escape of hydrogen. Tian (2015) find that as oxygen becomes the dominant species in the upper atmosphere, the Hunten et al. (1987) formalism predicts that an oxygen-dominated flow can rapidly lead to the loss of all O_2 from planets around M dwarfs. However, because of the larger mass of the oxygen atom, hydrodynamic oxygen-dominated escape requires exospheric temperatures $\sim m_O/m_H = 16$ times higher than that for a hydrogen-dominated flow, which is probably unrealistic for Proxima b. Following the prescription of Schaefer et al. (2016), we therefore shut off oxygen escape once its mixing ratio exceeds $X_O = 0.6$, switching to the diffusion-limited escape rate of hydrogen. Finally, as in Luger & Barnes (2015), we also consider the scenario in which sinks at the surface are efficient enough to remove O_2 from the atmosphere at the rate at which it is produced, resulting in an atmosphere that never builds up substantial amounts of oxygen. Recently, Schaefer et al. (2016) used a magma ocean model to calculate the rate of O_2 absorption by the surface, showing that final atmospheric O_2 pressures may range from zero to hundreds or even thousands of bars for the hot Earth GJ 1132b. Our two scenarios (no O_2 sinks and efficient O_2 sinks) should therefore bracket the atmospheric evolution of Proxima b.

3.3. Tidal Evolution: EQTIDE

To model the tidal evolution of the Proxima system, we will use a simple, but commonly-used model called the "constant-phase-lag" model (Goldreich 1966; Greenberg 2009; Heller et al. 2011). This model reduces the evolution to two parameters, the "tidal quality factor" Q and the Love number of degree 2, k_2. While this model has known shortcomings (Touma & Wisdom 1994; Efroimsky & Makarov 2013), it provides a qualitatively accurate picture of tidal evolution, and produces similar results as the competing constant-time lag model (Heller et al. 2010; Barnes et al. 2013; Barnes 2016). Moreover, Kasting et al. (1993) used CPL to calculate the "tidal lock radius." For this study, we use the model described in Heller et al. (2011), and validate it by reproducing the tidal evolution of the Earth-Moon orbit (MacDonald 1964) and the tidal heating of Io (Peale et al. 1979).

The values of Q and k_2 for Earth are well-constrained by lunar laser ranging (Dickey et al. 1994) to be 12 and 0.299, respectively (Williams et al. 1978; Yoder 1995). However, their values for celestial bodies are poorly constrained because the timescales for the evolution are very long. Values for stars are typically estimated to be of order 10^6 (*e.g.* Jackson et al. 2009); dry terrestrial planets have $Q \sim 100$ (Yoder 1995; Henning et al. 2009), and gas giants have $Q = 10^4 - 10^6$ (Aksnes & Franklin 2001; Jackson et al. 2008b). In § 4 we will consider the possibility that Proxima b began with a hydrogen envelope and was perhaps more like Neptune than Earth. There is some debate regarding the location of tidal dissipation in gaseous exoplanets, whether it is in the envelope (high Q) or in the core (low Q) (*e.g.* Storch & Lai 2014). We will consider planets with very thin hydrogen envelopes, so we will make this latter assumption and use the Q value computed by THERMINT (see § 3.7) for core-dominated cases.

3.4. Orbital Evolution: DISTORB

The model for orbital evolution, DISTORB (for "disturbing function orbit evolution"), uses the 4th order secular disturbing function from Murray & Dermott (1999) (see their Appendix B), with equations of motion given by Lagrange's planetary equations (again, see Murray & Dermott 1999). To avoid potential singularities in the equations of motion, we utilize the

variables

$$h = e \sin \varpi \tag{1}$$

$$k = e \cos \varpi \tag{2}$$

$$p = \sin \frac{i}{2} \sin \Omega \tag{3}$$

$$q = \sin \frac{i}{2} \cos \Omega, \tag{4}$$

rather than the standard osculating elements (e, i, ϖ, Ω). This variable transformation is straightforward, if tedious, so we do not reproduce it here. The resulting form of the disturbing function and Lagrange's equations will be explicitly stated in forthcoming works (Barnes et al., in prep, Deitrick et al., in prep). Lagrange's equations in this form can also be found in Berger & Loutre (1991).

We apply this model to the Proxima b and a possible longer period companion, hinted at in the RV data. This secular (*i.e.* long-term averaged) model does not account for the effects of mean-motion resonances; however, since we apply this to well-separated planets here, it is adequate for much of our parameter space. Since the model is 4th order in e and i, it can account for coupling of eccentricity and inclination, although it does begin to break down at higher eccentricity or mutual inclination. In Fig. 2 we compare our model to the HNBody[2] integrator (Rauch & Hamilton 2002) and find that for modest values of e and i the two methods are nearly indistinguishable.

3.5. Rotational Evolution from Orbits and the Stellar Torque: DISTROT

The planetary obliquity is a primary driver of climate, and hence we also track planet b's evolution carefully. Not only is it responsible for seasons, but a non-zero obliquity can result in tidal heating (Heller et al. 2011), which can change outgassing rates and atmospheric properties. Proxima b's obliquity is affected by two key processes: tidal damping and perturbations from other planets. The EQTIDE module handles the former, DISTROT the latter.

Our obliquity evolution model, DISTROT (for "disturbing function rotation evolution"), uses the equations of motion developed in Kinoshita (1975, 1977) and utilized in numerous studies including Laskar (1986), Laskar et al. (1993a,b), and Armstrong et al. (2014). It treats the planet as an oblate spheroid (having an axisymmetric equatorial bulge), with a

---

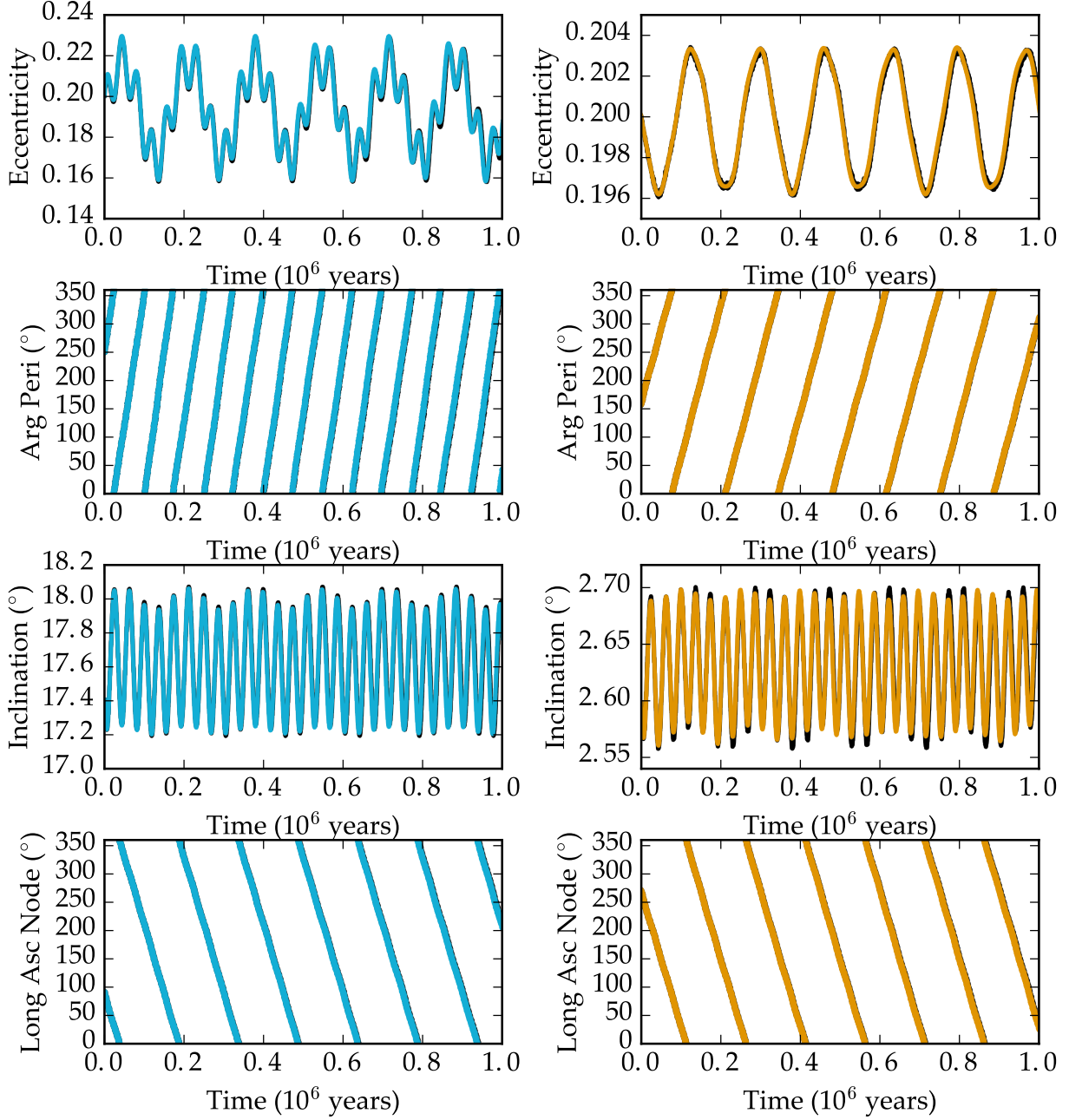[2]Publicly available at https://janus.astro.umd.edu/HNBody/

Fig. 2.— Comparison between the DISTORB module and the N-body code HNBody for the high e, i case in Table 1. Planet b is represented on the left, putative planet c on the right. HNBody evolution is in black, DISTORB in blue for planet b, orange for planet c.

shape controlled by the rotation rate (see below). The planet then is subject to a torque from the host star, which causes axial precession, and changes in its orbital plane due to perturbations from a companion planet, which directly change the obliquity angle. This model is thus dependent on DISTORB through the eccentricity, the inclination, the longitude of ascending node (Ω), and the derivatives $dp/dt, dq/dt$ (Eqs. 3 and 4).

The equations for obliquity and precession angle ($d\psi/dt, dp_A/dt$), also contain a singularity at $\psi = 0$, so we transform to the variables

$$\xi = \sin\psi \sin p_A \tag{5}$$
$$\zeta = \sin\psi \cos p_A \tag{6}$$
$$\chi = \cos\psi. \tag{7}$$

The third variable, χ, is necessary to preserve domain information. Hence, we ultimately have three variables to integrate rather than two.

Since we couple obliquity evolution in DISTROT to tidal evolution in EQTIDE, it is necessary to account for changes in the planet's shape (its dynamical ellipticity) as its rotation rate changes due to tides. Following the examples of Atobe & Ida (2007) and Brasser et al. (2014), we scale the planet's oblateness coefficient, J_2 (from which the dynamical ellipticity, E_d, can be derived), with the radius R_p, rotation rate ω_{rot}, and mass M, as

$$J_2 \propto \frac{\omega_{rot}^2 R_p^3}{M}. \tag{8}$$

We use the Earth's J_2 as a proportionality factor. As pointed out by Brasser et al. (2014), around a rotation period of 13 days, J_2 calculated in this way reaches the J_2 of Venus, which maintains this shape at a much slower rotation speed, and so, following their example, we set the minimum J_2 value to the J_2 of Venus.

In the presence of strong tidal effects, as we would expect at Proxima b's orbital distance, the obliquity damps extremely quickly (in a few hundred kyr). However, if another planetary mass companion is present, then gravitational perturbations can prevent the obliquity from damping completely. Furthermore, this equilibrium configuration, called a Cassini state, is confined to a configuration in which the total angular momentum vector of the planetary system, $\hat{k}$, the rotational angular momentum vector of the planet, $\hat{s}$, and the planet's own orbital angular momentum vector, $\hat{n}$, all lie in the same plane (Colombo 1966).

To identify Cassini states, we use the formula

$$\sin\Psi = \frac{(\hat{k} \times \hat{n}) \times (\hat{s} \times \hat{n})}{|\hat{k} \times \hat{n}|\,|\hat{s} \times \hat{n}|}, \tag{9}$$

suggested by (Hamilton & Ward 2004). In a Cassini state, the Ψ will oscillate (with small amplitude) about $0°$ or $180°$, so $\sin\Psi$ will approach zero. We will refer to $\sin\Psi$ as the "Cassini parameter". If a planet is in a Cassini state, its obliquity cannot be damped to 0.

3.6. Radiogenic Heating: RADHEAT

The first of two geophysical modules tracks the abundances of radioactive elements in the planet's core, mantle and crust. We consider 5 radioactive species: ^{26}Al, ^{40}K, ^{232}Th, ^{235}U, and ^{238}U. These elements have measured half-lifes of 7.17×10^5, 1.251×10^9, 1.405×10^{10}, 7.038×10^8, and 4.468×10^9 years, respectively. The energy associated with each decay is 6.415×10^{-13}, 2.134×10^{-13}, 6.834×10^{-12}, 6.555×10^{-12} and 8.283×10^{-12} J, respectively.

We will consider four different abundance ratios. First, we consider an Earth-like case with standard abundance concentrations (*e.g.* Korenaga 2003; Arevalo et al. 2009; Huang et al. 2013). Note that geoneutrino experiments are able to measure the decay products of ^{232}Th and ^{238}U (Raghavan et al. 1998; Araki et al. 2005; Dye 2010).

The second case uses chondritic abundances, in which we augment the mantle's ^{40}K budget by a factor of 30 in number to match the potassium abundance seen in chondritic meteorites (Anders & Grevesse 1989; Arevalo et al. 2009). Such high potassium abundances could be present if the planet formed beyond the snowline where potassium, a volatile, is more likely to become embedded in solids.

The third case is a planet containing an initial abundance of 1 part per trillion (ppt) of ^{26}Al. If the planet formed within 1 Myr and the planetary disk was enriched by a nearby supernova, either by planetesimal accumulation or a direct collapse in the outer regions of Proxima's protoplanetary disk, then not all the ^{26}Al would have decayed. A planet that formed quickly would likely have more than 1 ppt of ^{26}Al, but as we will see in § 4, but this case provides an end-member case for copmarison. The decay of ^{26}Al at $t = 0$ produces enough heat to melt 1 g of a CI meteorite, preventing their solidification for several half-lives (Hevey & Sanders 2006). Note that Earth required tens to hundreds of millions of years to form, so all the primordial ^{26}Al in the Solar System had already decayed.

The final case is an inert planet with no radioactive particles. This case is very unlikely in reality, but serves as a useful end-member case to bound the evolution of Proxima b.

3.7. Geophysical Evolution: THERMINT

We model the coupled core-mantle evolution of Proxima b with a 1-dimensional model that has been calibrated by modern-day Earth (Driscoll & Bercovici 2014; Driscoll & Barnes 2015); the reader is referred to those studies for a comprehensive description. Briefly, the model solves for the average core and mantle temperatures as determined by energy balance in the two layers and temperature-dependent parameterizations for heat loss. The code includes heat transport across the mantle-surface and core-mantle boundaries (CMB), mantle melt production and eruption rates, latent heat production by mantle and core solidification, and radiogenic and tidal heating; see § 3.3. Given the thermodynamic state of the core and the pressure of the stellar wind at the orbit of Proxima b, a magnetic moment scaling law is used to predict the core generated magnetic field and the resulting magnetopause radius. However, we note that the host star's strong magnetic field may compress the planet's magnetosphere close to its surface (Vidotto et al. 2013; Cohen et al. 2014).

Our model has been validated by reproducing the modern Earth's heat budget, mantle temperature and eruption flux, inner core radius, and magnetic moment. It has also been used to produce the divergent evolution of Venus and Earth under the assumption that they formed with similar compositions and temperatures, and that Venus has had a stagnant lid and Earth a mobile lid (Driscoll & Bercovici 2014). This model does require the calibration of some uncertain parameters (such as the lower mantle viscosity and core composition), and the assumption that Earth and Venus began with the same compositions. While this model is generic in many ways, it does assume an Earth-like composition, structure, mass and radius. The minimum mass for Proxima b is close enough to Earth's for this model to produce first order predictions for its thermal evolution. We note that THERMINT is limited to initial mantle temperatures above ∼1500 K, below which point differentiation may not occur, and below 8000 K, where additional phase changes would require additional physics.

The THERMINT modules can be directly coupled to EQTIDE as shown in Driscoll & Barnes (2015). In that case, we assume all the tidal power is deposited in the mantle and the heating changes the temperature, viscosity, and in turn the tidal Q. Driscoll & Barnes (2015) used a visco-elastic model in which the tidal heating reaches a maximum for mantle temperature near 1800 K, and thus cooling planets that pass through this temperature can experience a spike in tidal power generation.

3.8. Galactic Effects: GALHABIT

Proxima Centauri is tenuously bound, if it is gravitationally bound at all, to the binary α Cen A and B. Because of this, it is worthwhile to investigate the effects of the galactic environment on Proxima's orbit. We model the changes produced by galactic tides and stellar encounters using the equations and prescriptions developed to study the Oort cloud (Heisler & Tremaine 1986; Heisler et al. 1987; Rickman et al. 2008), as Proxima probably has a similar orbit about α Cen A and B. We utilize an updated galactic density of $\rho_0 = 0.102$ $M_\odot pc^{-3}$ (Holmberg & Flynn 2000) and treat α Cen A and B as a single point mass with $M = 2.1$ $M_\odot$ (with the recently updated masses given by Pourbaix & Boffin (2016)). This is a somewhat crude approach, as the two stars produce a significant quadrupole moment associated with their orbits—a back-of-the-envelope calculation indicates that the torque associated with this quadrupole potential would be equal to the galactic tidal torque at ~ 2000 AU. Hence, the effect of the binary host should be minor at Proxima's estimated distance of $\sim$15,000 AU. The importance is increased if Proxima has a significant eccentricity. However, the modeling of the triple system in a comprehensive way is sufficiently complicated (see, *e.g.* Harrington 1968; Ford et al. 2000) to place it beyond the scope of this work. Instead, we restrict ourselves to the secular effects of galactic tides and passing stars and will revisit the triple star dynamics in future work.

If Proxima is gravitationally bound, galactic tides and stellar encounters can pump its eccentricity to values large enough to cause disruption from the system, and/or a periastron distance so close to the binary α Cen that we would expect consequences for any planetary system, such as eccentricity excitation. In such situations, Proxima b may have significant tidal heating despite the circularization timescale.

Following Heisler et al. (1987) and Rickman et al. (2008), we model stellar encounters with a stochastic Monte Carlo approach, estimating times of encounters from the stellar density and velocity dispersion, and then randomly drawing stellar magnitudes and velocities from the distributions published in García-Sánchez et al. (2001). The impact parameter and velocity are calculated from the relative velocities (stellar velocity relative to the apex velocity, see Rickman et al. (2008)), and then a Δv is applied to Proxima's orbit according to the impulse approximation (Remy & Mignard 1985). The masses of passing stars are calculated using the empirical relations from Reid et al. (2002).

As previously noted, the metallicities of α Cen A and B suggest that the system formed at a galactocentric distance of $\lesssim 4.5$ kpc (Loebman et al. 2016). To model the potential effects of radial migration on the triple star system (again, assuming Proxima is gravitationally bound to A and B), we scale the stellar density and gas density of the galaxy according to the radial scale lengths $(R_\star, R_{gas})$ found by Kordopatis et al. (2015). The dark matter

density at each distance is estimated from their spheroidal model—unlike the disk models used for stars and gas, this model is not axisymmetric. However, as the dark matter near the mid plane of the disk makes up $\lesssim 1\%$ of the total density, it is a decent approximation to assume axisymmetry of the total mass density, as the Heisler & Tremaine (1986) tidal model assumes. We scale the velocity dispersions of the nearby stars as a decaying exponential with twice the stellar scale length, $2R_\star$, multiplied by $\sqrt{t}$, where t is the time since galactic formation, as found to be broadly true in galactic simulations (Minchev et al. 2012; Roškar et al. 2012). In this fashion, the velocity dispersion grows slowly in time at all galactic radii, and it grows larger closer to the galactic center. The apex velocity, *i.e.* the velocity of the star with respect to the Local Standard of Rest, will vary according to the detailed orbital motion of Proxima through the galaxy, including the radial migration. For the purposes of this study, we simply keep the apex velocity constant, assuming the current Solar value is typical, and we will revisit this problem in a later study.

With such scaling laws in place, we model radial migration as a single, abrupt jump in the galactocentric distance of the system. The reasoning behind this approximation is that N-Body simulations show migration to occur generally over the course of a single galactic orbit (Roskar 2010); hence, the migration time is short compared to the age of the stellar system. We then randomly choose formation distances over the range $(1.5, 4.5)$ kpc and migration times over the range $(1, 5)$ Gyr since formation.

3.9. The Coupled Model: VPLANET

The previously described modules are combined into a single software program called VPLANET. This code, written in C, is designed to be modular so that for any given body, only specific modules are applied and specific parameters integrated in the forward time direction. Parameters are integrated using a 4th order Runge-Kutta scheme with a timestep equal to η times the shortest timescale for all active parameters, *i.e.* $x/(dx/dt)$, where x is a parameter. In general, we obtain convergence if $\eta \leq 0.01$. A more complete and quantitative description of VPLANET will be presented soon (Barnes et al., in prep.).

Each individual model is validated against observations in our Solar System or in stellar systems. When possible, conserved quantities are also tracked and required to remain within acceptable limits. With these requirements met, we model the evolution of Proxima Centauri b for plausible formation models to identify plausible evolutionary scenarios, focusing on cases that allow the planet to be habitable. As Proxima b is near the inner edge of the HZ, we are primarily concerned with transitions into or out of a runaway greenhouse. For water-rich planets, this occurs when the outgoing flux from a planet is ~ 300 W/m^2 (Kasting

et al. 1993; Abe 1993) and for dry planets it is at 415 W/m^2 (Abe et al. 2011). For water-rich planets, we use the relationship between HZ limits, luminosity and effective temperature as defined in Kopparapu et al. (2013).

4. Results

4.1. Galactic Evolution

If Proxima is or was bound to α Cen A and B, then Proxima's orbit may be modified by the galactic tide and perturbations from passing stars. We ran two experiments to explore the effects of radial migration: set **A** places the system in the solar neighborhood, randomly selecting orbital parameters broadly consistent with the observed positions, for 10,000 trials. In set **B**, we have taken the same initial conditions and randomly selected formation distances over the range [1.5,4.5] kpc (Loebman et al. 2016) and migration times over (1,5) Gyr after formation, after which the system is moved to the solar neighborhood (8 kpc).

Simulations were halted whenever Proxima's orbit passed within 40 AU of the center of mass of α Cen A and B, when it passed beyond 1 pc, or when it became gravitationally unbound ($e > 1$). In set **A** (see Figure 3), 1506 out of 10,000 simulations were halted because of one of the three above conditions. Closer inspection reveals that the majority of these (1289) were halted because Proxima's periastron passed within 40 AU of α Cen. Of those that didn't halt, another 1363 passed within 200 AU and 620 passed within 100 AU. Including those trials that were halted for any reason, 2688 (27%) passed within 200 AU and 1929 (19%) passed within 100 AU.

The importance of this distance is that ~ 100 AU is the distance a close encounter with a $\sim 2\,M_\odot$ star would disrupt a planetary system similar to the solar system (Kaib et al. 2013). The fact that α Cen is a binary itself, with a large eccentricity ($e \sim 0.5$) probably increases the disruption distance still further. Of course, Proxima is very different from the Sun and may never have formed a planetary system like the one we inhabit (with gas giants at large orbital distances); however, it may still have had an extended planetary system at some point. If that is the case, the system may have been disrupted, or may be disrupted in the future, by a close periastron passage with α Cen. Proxima b may be the remnant of a more extended planetary system that experienced such a disruption. Or, if additional planets remain in the system, *future* close encounters with α Cen A and B could cause instabilities and chaos within the planetary system, so the future evolution should also be considered for its long-term habitability.

Radial migration, set **B**, makes close passages and disruption more likely, as shown in

Fig. 3. In this set, 2544 trials were halted and 1717 of those were due to periastron reaching below 40 AU. Of the remaining cases, 1333 had periastron distances < 200 AU and 634 below < 100 AU. Including cases that were halted, 3195 (32%) passed within 200 AU and 2452 (25%) passed within 100 AU. An example of the orbital evolution of Proxima with radial migration is shown in Fig. 6.

One potential issue with our orbit-averaged approach is that for Proxima in the semi-major axis range (~ 5000 to ~ 20000) AU, the orbital periods span a range of 240 thousand to 2 million years. Thus it may be possible in the simulations for Proxima's periastron to come very close to α Cen for a short period of time and then evolve to a larger distance before Proxima ever *actually reaches* periastron. Hence, we are potentially halting simulations in which Proxima may not actually pass within 40 AU of α Cen. Our results should thus be seen as an upper limit on the number of configurations that lead to close encounters between Proxima and α Cen.

4.2. Orbital/Rotational/Tidal Evolution

We begin exploring the dynamical properties of the orbits and spins by considering the tidal evolution of Proxima b if it is in isolation. In this case, we need only apply EQTIDE to both Proxima and b and track a, e, P_{rot}, and ψ. We find that if planet b has $Q = 12$, then an initially Earth-like rotation state becomes tidally locked in $\sim 10^4$ years, so it seems likely that if b formed near its current location, then it formed in a tidally locked state and with negligible obliquity.

Unlike the rotational angular momentum, the orbit can evolve on long timescales. In the top two panels of Fig. 7, we consider orbits that begin at $a = 0.05$ AU and with different eccentricities of 0.05 (dotted curves), 0.1 (solid curves) and 0.2 (dashed curves). In these cases a and e decrease and the amount of inward migration depends on the initial eccentricity, which takes 2–3 Gyr to damp to ~ 0.01. For initial eccentricities larger than ~ 0.23, the CPL model actually predicts eccentricity growth due to angular momentum exchange between the star and planet (Barnes 2016). This prediction is likely unphysical and due to the low order of the CPL model; therefore we do not include evolutionary tracks for high eccentricities.

The equilibrium tide model posits that the lost rotational and orbital energy is transformed into frictional heating inside the planet. The bottom panel of Fig. 7 shows the average surface energy flux as a function of time. We address the geophysical implications of this tidal heating in § 4.5.2. Note that if planet b begins with a rotation period of 1 day and an
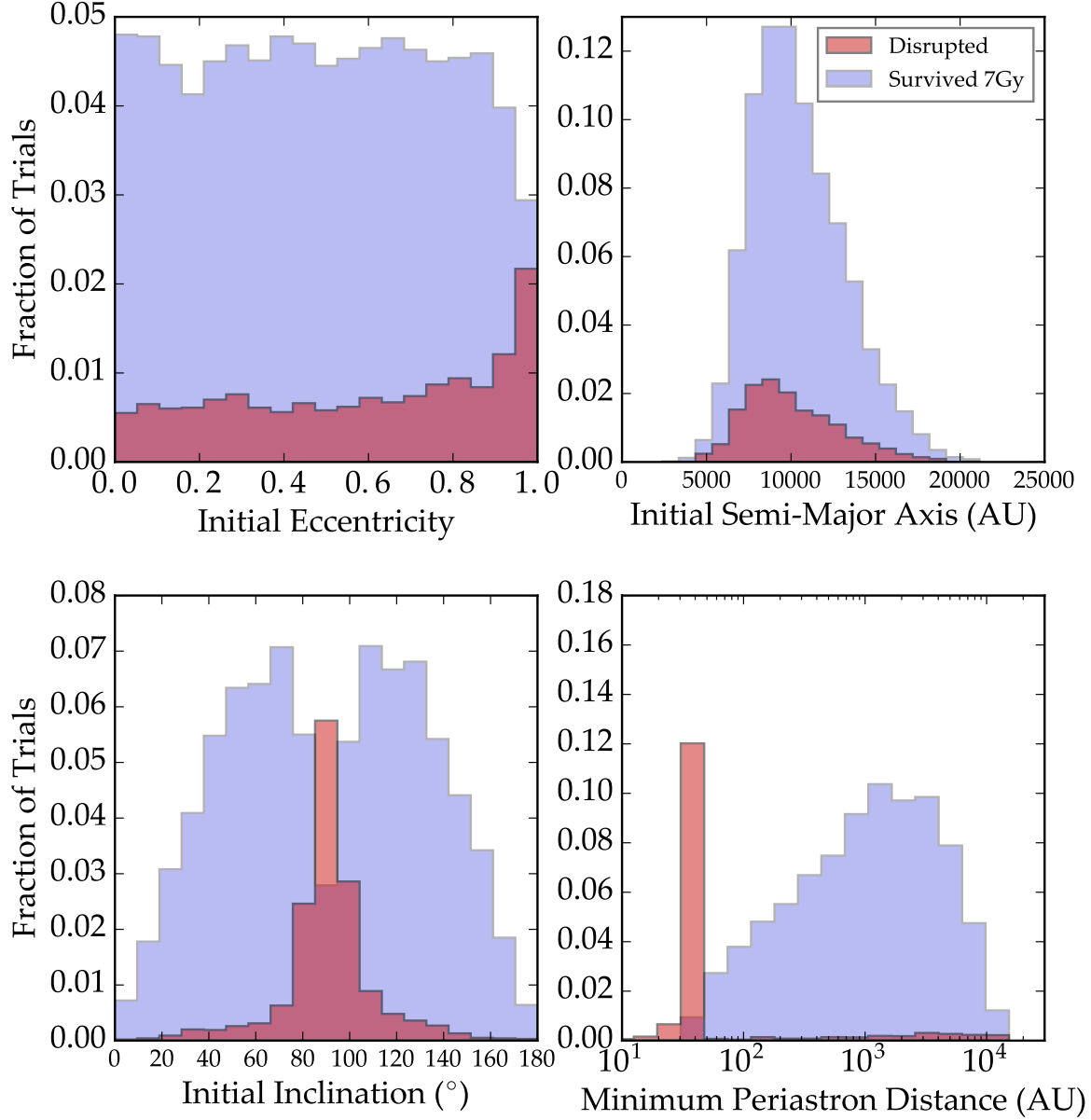
Fig. 3.— Stability of Proxima Cenaturi's orbit without radial migration. Distributions of trials in which Proxima's orbit about α Cen is disrupted (red) and trials in which it survives to greater than the age of the system (blue). *Top left:* Initial eccentricity. *Top right:* Initial semi-major axis. *Bottom left:* Initial inclination relative to the galactic disk. *Bottom right:* Minimum periastron distance over the entire simulation. Generally, eccentricity and inclination are the greatest determinants of stability, with high e and $i \sim 90°$ (*i.e.* low $\hat{Z}$-angular momentum) cases being the least stable. Amongst the cases we considered "stable," a significant fraction still have Proxima passing within a few hundred AU of α Cen A and B.
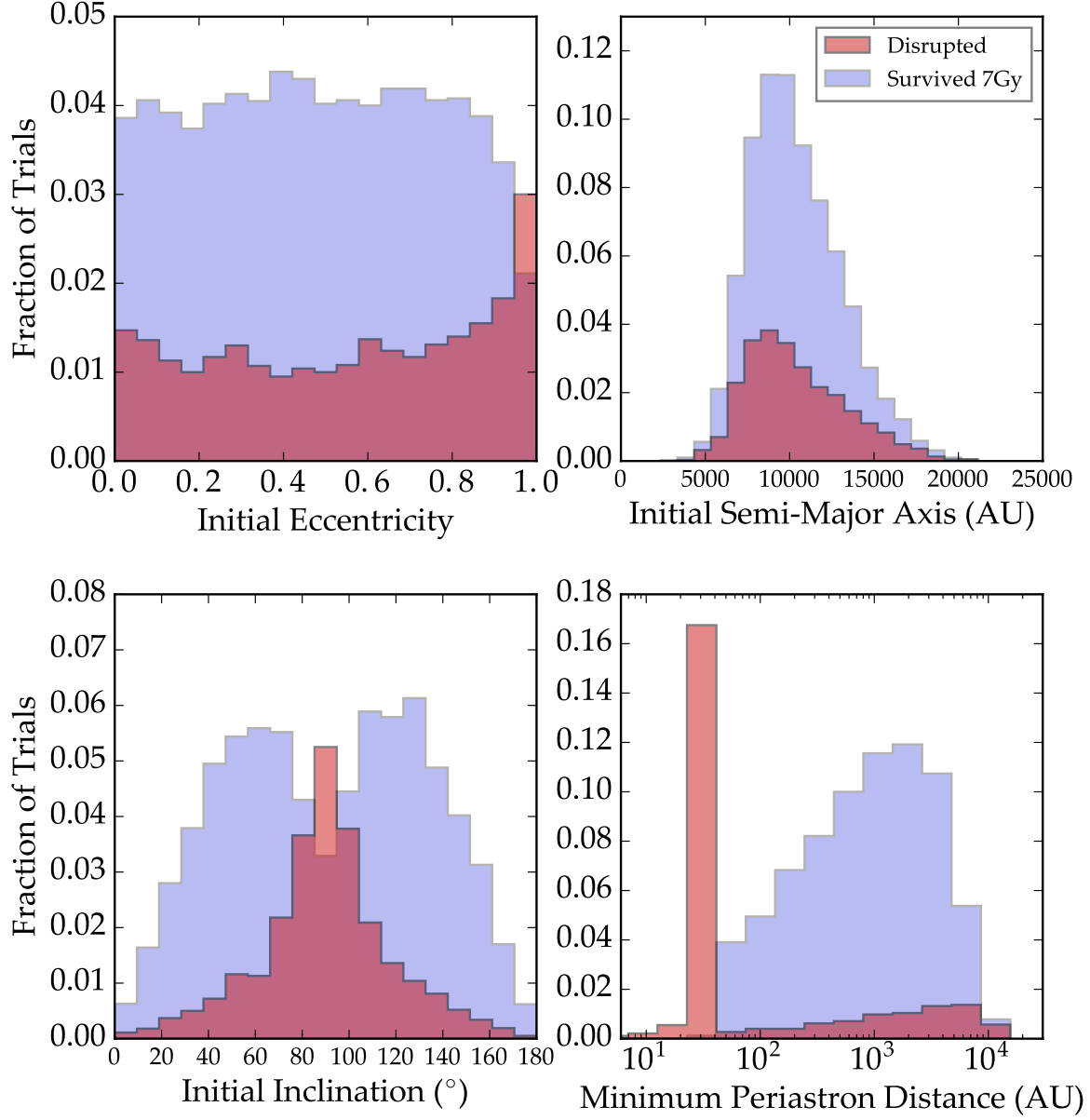
Fig. 4.— Same as Fig. 3 but with radial migration. Systems which formed interior to 4.5 kpc from the galactic center are disrupted more frequently than those which were placed in the solar neighborhood from the beginning.
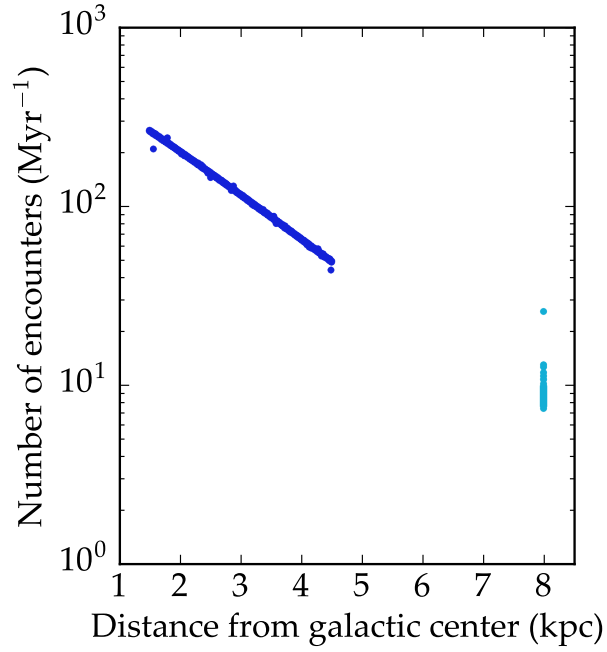
Fig. 5.— Stellar encounter rates as a function of galactocentric distance. Dark blue points correspond to pre-migration encounter rates, light blue to post-migration. The large outlier in the solar-neighborhood is due to small number statistics—the system in that simulation was disrupted shortly after migration. There is some scatter in the solar-neighborhood points because of the time dependence of the stellar velocity dispersion. At the tail end of the simulations, we match the encounter frequency of 10.5 Myr^{-1} from previous studies (García-Sánchez et al. 2001; Rickman et al. 2008).
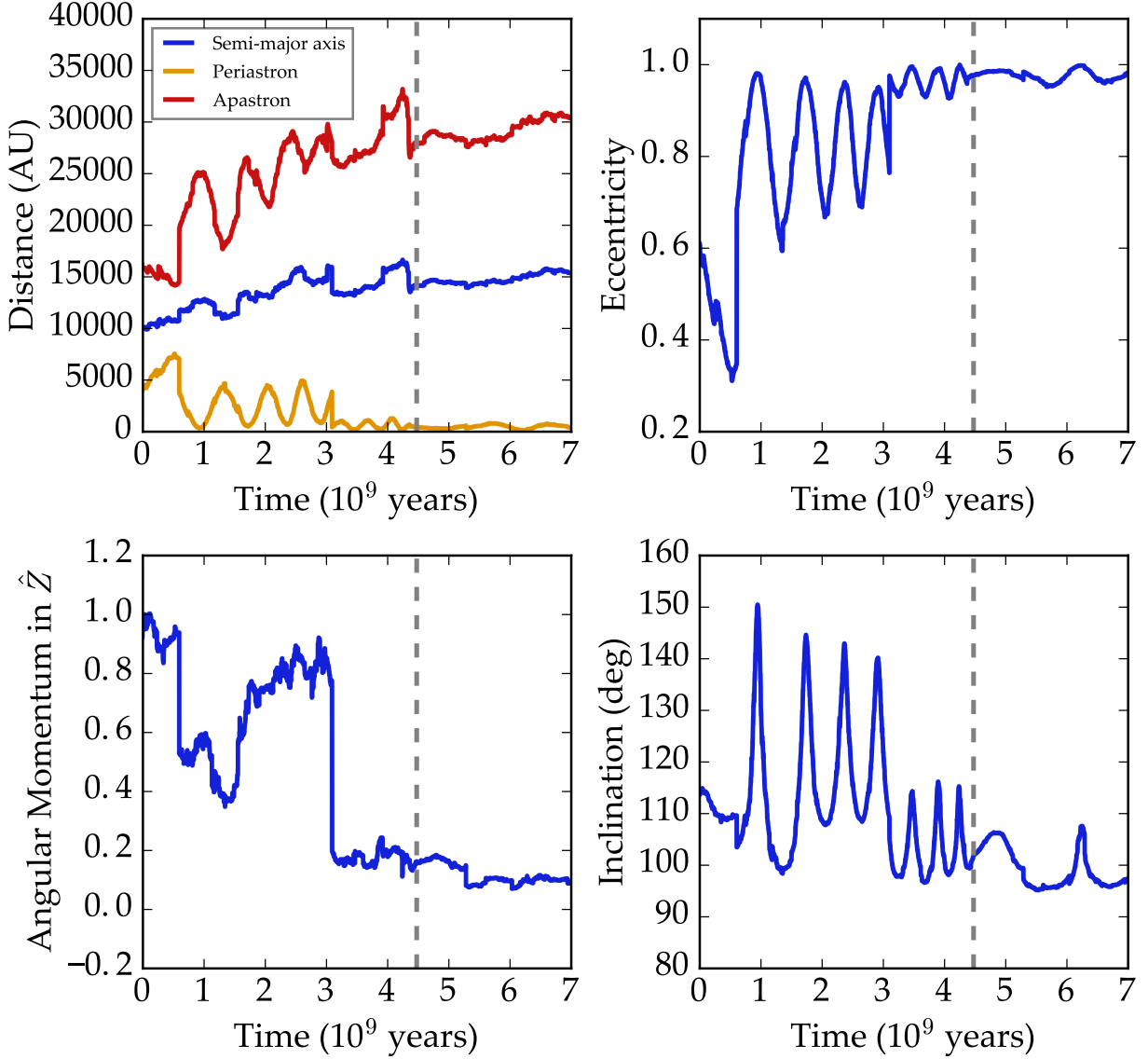
Fig. 6.— An example of the orbital evolution of Proxima in the galactic simulations. The upper left panel shows the semi-major axis, periastron distance, and apastron distance, the upper right shows the eccentricity, the lower left shows the angular momentum in the $\hat{Z}-$direction, and the lower right shows the inclination with respect to plane of the galactic disk. The system was given a formation distance of $R = 3.78$ kpc and the vertical dashed line shows the time of migration (to 8 kpc). The angular momentum in $\hat{Z}$ (the action J_z) is unchanged by galactic tides—eccentricity and inclination exchange angular momentum in such a way that this quantity is conserved—thus its evolution is purely due to stellar encounters. In this particular case, the eccentricity of Proxima grows such that its periastron dips within 50 AU of α Cen A and B.

obliquity of 23.5°, then the initial surface energy flux due to tidal heating is $\sim$ 1 kW/m^2.

Next, we consider the role of additional planets, specifically the putative planet with a 215 day orbit (Anglada-Escudé 2016). For these runs we now add the DISTORB and DISTROT modules and track the orbital elements of both planets, the spins of the star and planet b, and the dynamical ellipticity of planet b. A comprehensive exploration of parameter space is beyond the scope of this study, so we consider two end-member cases: a nearly coplanar, nearly circular system, and a system with high eccentricities and inclinations. The initial orbital elements and rotational properties of the bodies are listed in Table 1.

	m ($M_\oplus$)	a_s (au)	a_l (au)	e	i (°)	ω (°)	Ω (°)	ψ (°)	P_{rot} (days)
b	1.27	0.0482817	0.05	0.001	0.001	248.87	20.68	23.5	1
c	3.13	0.346	0.346	0.001	0.001	336.71	20		
b	1.27	0.0482817	0.05	0.02	20	248.87	20.68	23.5	1
c	3.13	0.346	0.346	0.02	0.001	336.71	20		

Table 1: Initial conditions for Proxima 2-planet systems. The coplanar, circular case is on top, the eccentric, inclined case below.

In Fig. 8 we show the orbital evolution for the low e and i case over short (left) and long (right) timescales. As expected, the planets exchange angular momentum, but over the first million years there is no apparent drift dueto tidal effects. On longer timescales, however, we see the eccentricity of b slowly decay due to tidal heating. Note the differences in timescale for the decay between Figs. 7 and 8. The perturbations from a hypothetical "planet c" maintain significant eccentricities for long periods of time.

In Fig. 9, we plot the orbital evolution for the high e and i case. The eccentricity and inclination oscillations are longer, and the eccentricity cycles show several frequencies due to the activation of higher order terms in the coupling coupling of e and i. As in the low e and i case, the eccentricity damps more slowly than in the unperturbed case. Note as well that the inclination oscillation amplitude decays with time.

In Fig. 10, we plot the evolution of the rotational parameters for the two cases. In the top left panel, we show the evolution of the rotational period. The rotation becomes tidally locked very quickly (less than 1 Myr for all plausible values of Q for an ocean-bearing world). In the high e, i case, the planet briefly enters the 3:2 spin orbit resonance (like the planet Mercury). The obliquity initially grows due to conservation of angular momentum (Correia et al. 2008), but then damps down. For the high e, i case, the obliquity reaches an equilibrium
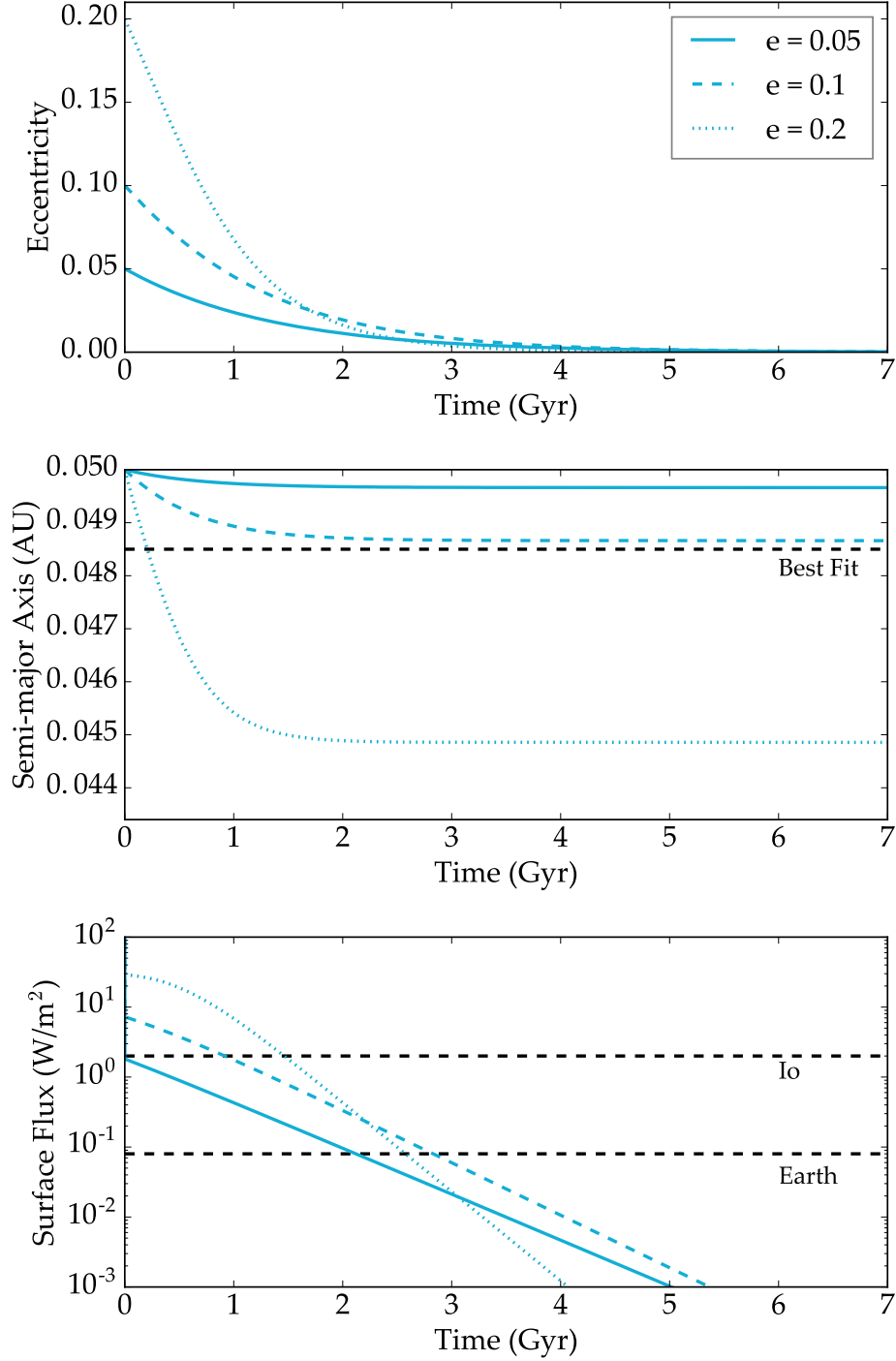
Fig. 7.— Evolution of planet b's eccentricity (top), semi-major axis (middle), and tidal heating surface flux (bottom) assuming that initially $a = 0.05$ AU and $e = 0.05$ (dotted), 0.1 (solid) or 0.2 (dashed). For reference the best fit semi-major axis and surface energy fluxes of Io and the modern Earth are shown by dashed black lines.
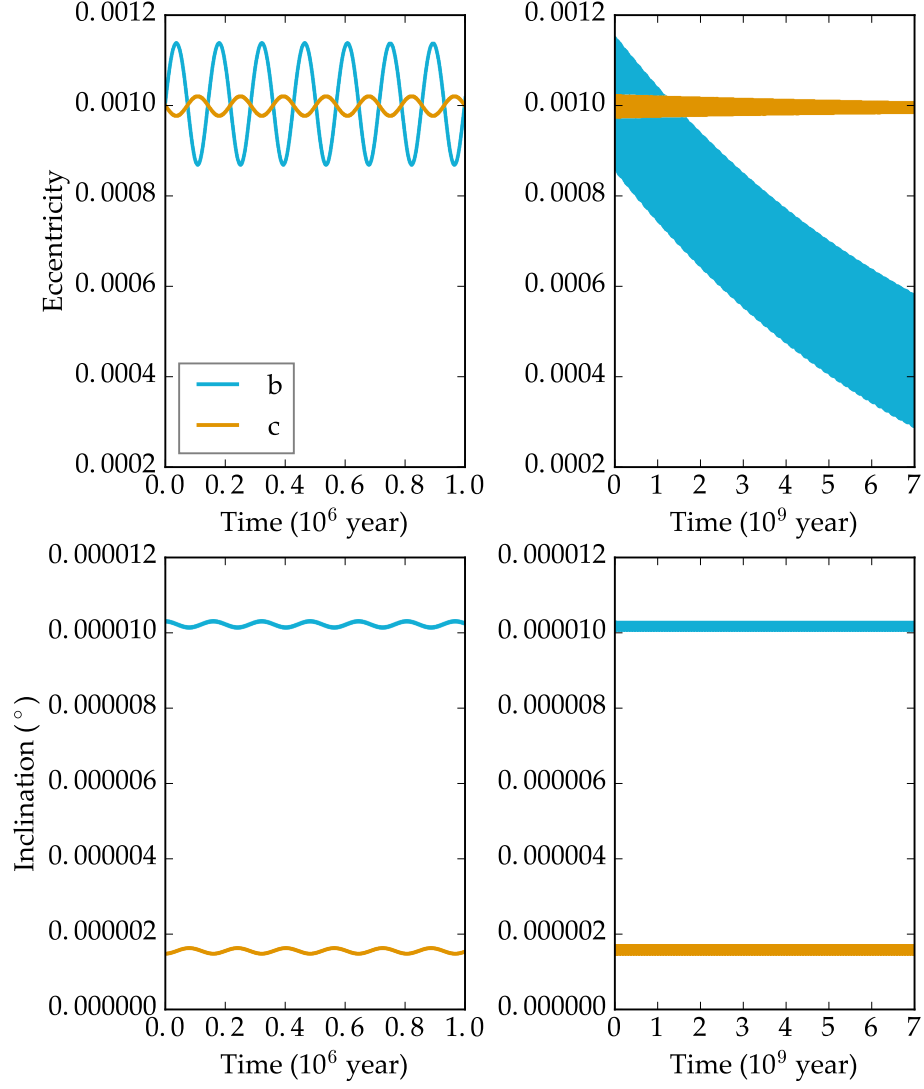
Fig. 8.— Evolution of orbital elements if a putative planet c exists with an orbital period of 215 days and both orbits are nearly circular and nearly coplanar. *Top Row:* Eccentricity. *Bottom Row:* Inclination.
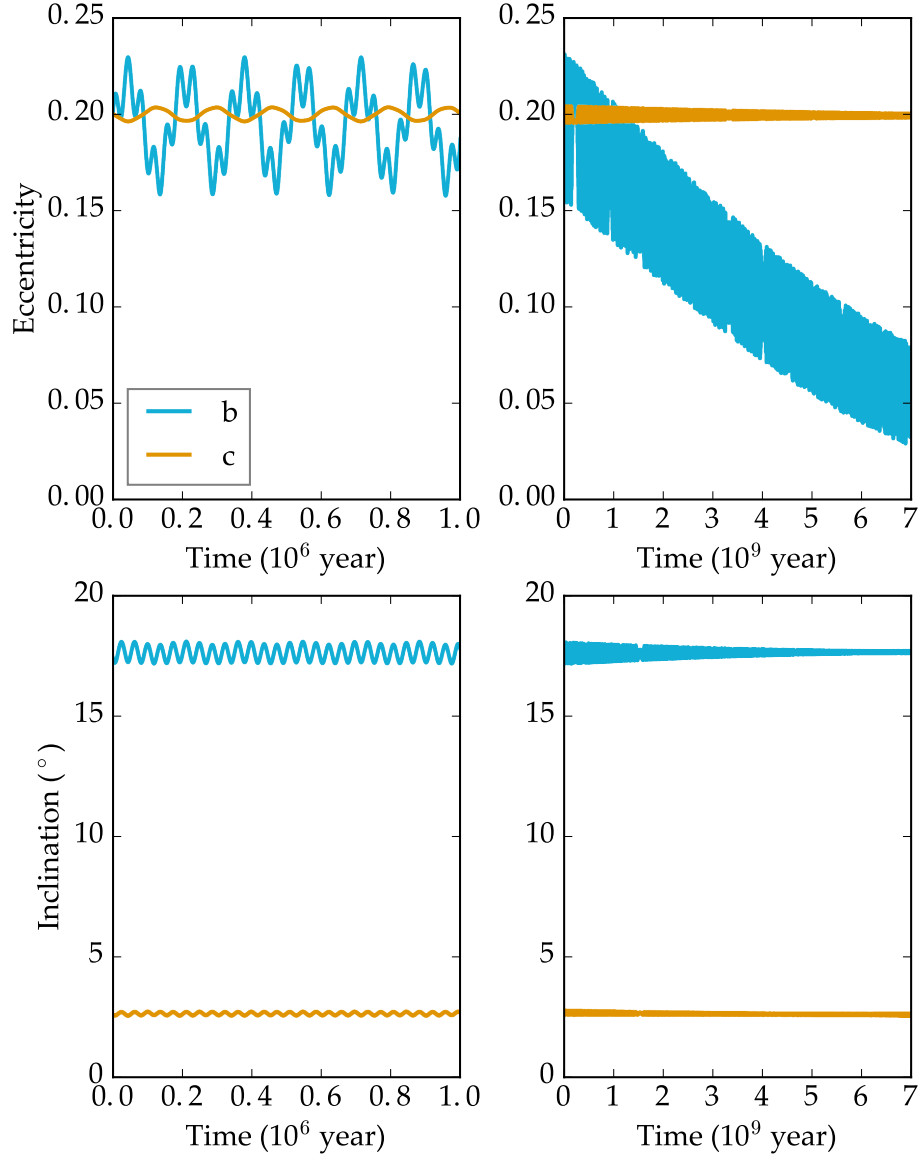
Fig. 9.— Same as Fig. 8, but for the high e, i case.

value near $0.1°$, while the low e, i case drops all the way to 10^{-8} $°$. The bottom left panel shows the evolution of the dynamical ellipticity as predicted by the formulae from Atobe & Ida (2007). Realistically, the shape of the planet should lag this shape by a timescale dependent on the planet's rigidity, but we ignore that delay here. The lower right panel shows the value of the Cassini Parameter (see Equation 9) for the two cases, both of which becomes locked near zero, indicating the rotational and angular momentum have evolved into a Cassini state (in this case, Cassini state 2), in which the spin and orbit vectors of planet b are on opposite sides of the total angular momentum vector of the planetary system.

4.3. Stellar Evolution

In Fig. 11 we plot the evolution of the conservative HZ limits of Kopparapu et al. (2013) (blue region) as a function of time; the HZ is bounded by the runaway greenhouse limit on the side closest to the star and by the maximum greenhouse limit on the opposite side. Because of the pre-MS luminosity evolution of Proxima, the HZ slowly moves inward for $\sim$ 1 Gyr, reaching the current orbit of Proxima b after $\sim$ 160 Myr.

The figure also shows the "dry" HZ limits of Abe et al. (2011), which apply to planets with very limited surface water ($\lesssim 1\%$ of the Earth's water inventory); these planets are significantly more robust to an instellation-triggered runaway. Consequently, if Proxima b's initial water content was very low, it would have spent significantly less time in a runaway greenhouse. However, a dry formation scenario for Proxima b does not help its present-day habitability. As we show in §4.4, Proxima b loses 1 ocean of water in $\lesssim 4$ Myr; if it formed with less water than that, it would be completely desiccated long before entering the Abe et al. (2011) HZ. One can envision cases in which the planet forms dry but with a protective hydrogen envelope, or forms after ~ 10 Myr, but such scenarios are unlikely *a priori* and hence we do not consider them here.

In the atmospheric escape section below, we thus use a value of 160 Myr for the duration of the runaway greenhouse phase on Proxima b, during which time water is allowed to escape.

4.4. Atmospheric Evolution

We consider two broad formation scenarios for Proxima b: one in which it formed with abundant water and a thin hydrogen envelope of up to 1% by mass (due to either *in situ* accretion or from planetary formation farther out followed by rapid disk-driven migration; see Luger et al. (2015)), and one in which it formed with abundant water but no hydrogen.
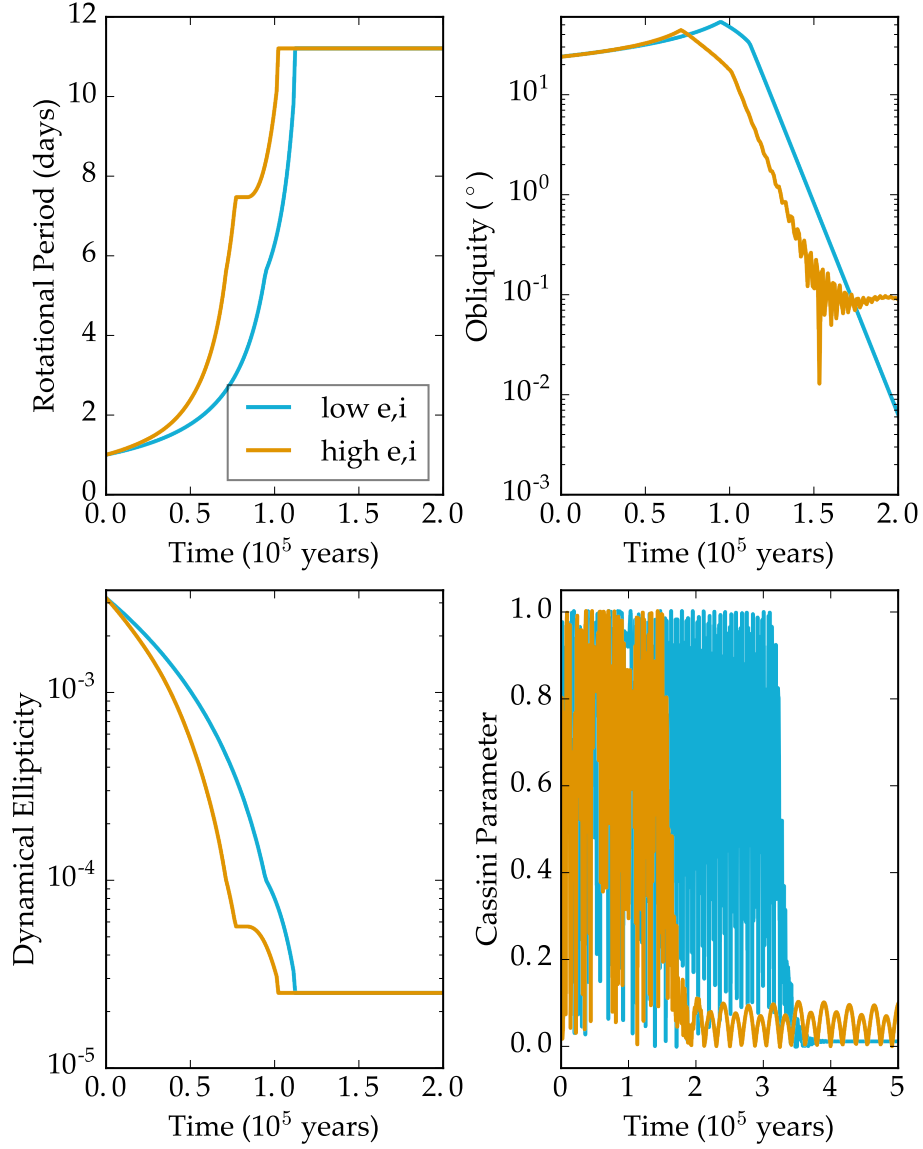
Fig. 10.— Evolution of rotational properties of planet b for the two hypothetical multiplanet systems, with the low e, i case in blue, and high e, i case in orange. *Top left:* Rotation Period. *Top right:* Obliquity. *Bottom left:* Dynamical Ellipticity. *Bottom right:* Cassini Parameter.
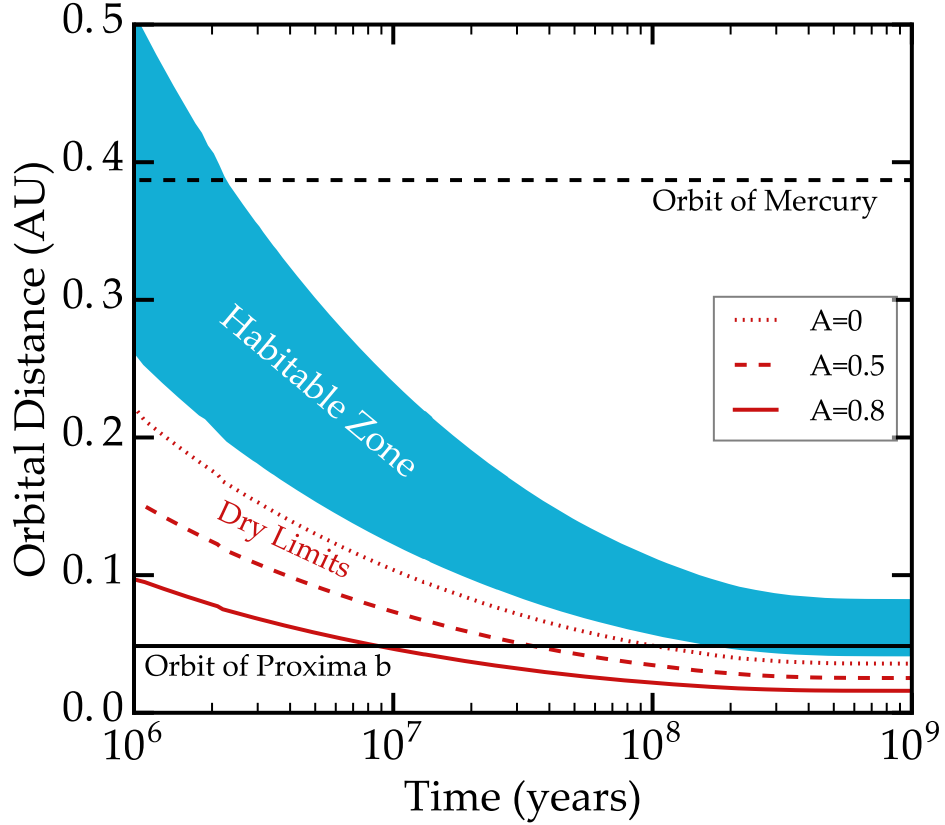
Fig. 11.— Evolution of the HZ of Proxima Centauri, along with the orbits of Proxima Centauri b (solid line) and Mercury (dashed line). The blue region is the conservative HZ of Kopparapu et al. (2013), while the red lines are the HZ limits for dry planets of different albedos, A, from Abe et al. (2011).

In both cases, we assume a fiducial planet mass of $1.27\,\mathrm{M_\oplus}$.

In Fig. 12 we show the evolution of the latter type of planet, which formed with no significant primordial envelope. We consider four different initial inventories of water: 1, 3, 5, and 10 terrestrial oceans (1 TO $\equiv 1.39 \times 10^{24}$ g, the total mass of surface water on Earth; see Kasting (1988)). As discussed in § 3.2, we also consider two end-member scenarios regarding the photolytically-produced O_2: no surface sinks (solid lines) and efficient surface sinks (dashed lines). In all cases but one, the planet is completely desiccated within the first 160 Myr, building up between tens and hundreds of bars of O_2 in either its atmosphere or in the solid body. For an initial water content of 10 TO and no surface sinks, O_2 builds up to high enough levels to throttle the supply of H to the upper atmosphere and slow the total escape rate. In this scenario, ~ 1 TO of water remains, alongside a thick 500 bar O_2

atmosphere. If Proxima b formed with less than ten times Earth's water content, and/or had a persistent convecting, reducing magma ocean, it is likely desiccated today.

Next, in Fig. 13, we show the results assuming Proxima b formed with a hydrogen envelope. We fix the initial water content at 3 TO and consider initial envelope mass fractions f_H ranging from 10^{-4} to 10^{-2}. In all cases, the envelope evaporates completely within the first several hundred Myr. For $f_H \lesssim 10^{-3}$, the envelope evaporates early enough such that all the water is still lost from the planet. For $f_H = 10^{-3}$, only about 0.1 TO remain once the planet enters the HZ; only for $f_H \sim 10^{-2}$ does the presence of the envelope guard against all water loss. In these calculations, we assumed inefficient surface sinks, so the escape of water at late times was bottlenecked by the presence of abundant O_2. Planets that form with hydrogen envelopes may have quite reducing surfaces, which could absorb most of the O_2 and lead to even higher total water loss. As before, a few tens to a few hundreds of bars of O_2 remain in the atmosphere or in the solid body at the end of the escape phase.

We note that we obtain slightly more hydrogen loss than Owen & Mohanty (2016), who find that planets more massive than $\sim 0.9\,\mathrm{M_\oplus}$ with $\sim 1\%$ hydrogen envelopes cannot fully lose their envelopes around M dwarfs, due primarily to the transition from hydrodynamic to ballistic escape at late times. However, their calculations were performed for a $0.4\,\mathrm{M_\odot}$ M dwarf, whose pre-main sequence phase lasts $\sim 200\mathrm{Myr}$, five times shorter than that for Proxima Centauri. Nevertheless, the discrepancy is small: we find that for envelope fractions greater than 1% or masses greater than our fiducial value of $1.27\,\mathrm{M_\oplus}$, the envelope does not completely evaporate, in which case Proxima b would likely be uninhabitable.

Finally, in Figs. 14–15 we present a summary of our atmospheric escape calculations, showing the many possible evolutionary pathways for Proxima b and how they affect its present habitability. The two panels show the final water content (in TO) versus the final oxygen abundance (in bars) for different initial conditions, assuming inefficient oxygen sinks (Figs. 14) and efficient oxygen sinks (Figs. 15). In all cases shown, the final hydrogen envelope mass is zero. Different values of the planet mass, initial water content, and hydrogen fraction are indicated with different marker styles (see legend at right). Since the axes are logarithmic, we appended panels to the left and below the main plot, corresponding respectively to final oxygen and water contents of zero. In general, habitable outcomes are those that lie in the top left of the plot (abundant water, low O_2). Planets in the top right have abundant water but also build up large amounts of O_2, which could render them uninhabitable (Luger & Barnes 2015) and/or fool observers searching for biosignatures (Schwieterman et al. 2016). Planets at the bottom of the plot are desiccated and therefore uninhabitable, though some may also be biosignature false positives.

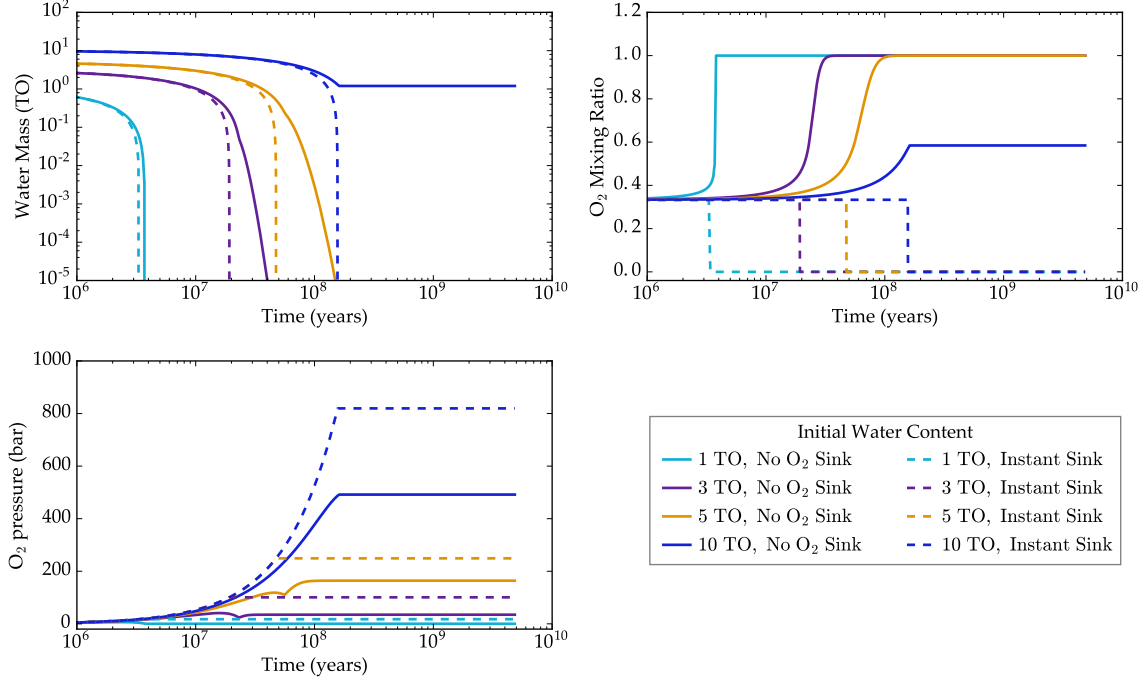While much may be gleaned from the figure, a few results stand out. First, a scenario in

– 38 –

Fig. 12.— Evolution of the water content and atmospheric O$_2$ pressure on Proxima b for different initial conditions. The initial water content is varied between 1 and 10 TO (various colors) for two different end-member scenarios: no O$_2$ surface sinks (solid lines) and instantaneous oxygen absorption at the surface (dashed lines). The planet mass is held constant at 1.27 M$_\oplus$ and the initial hydrogen envelope fraction is set to zero for all runs. In all but one of the runs, Proxima b is completely desiccated. For an initial water content of 10 TO and no surface sinks, the buildup of $\sim$ 500 bars of atmospheric O$_2$ slows the loss rate of H, preventing the last $\sim$ 1 TO of water from being lost. In the scenario that efficient oxygen sinks are present, the atmospheric O$_2$ mixing ratio never grows sufficiently to limit the escape of H, and desiccation occurs in all cases. Note that in this scenario, the curves in the "O$_2$ pressure" panel correspond to the equivalent O$_2$ pressure absorbed at the surface.
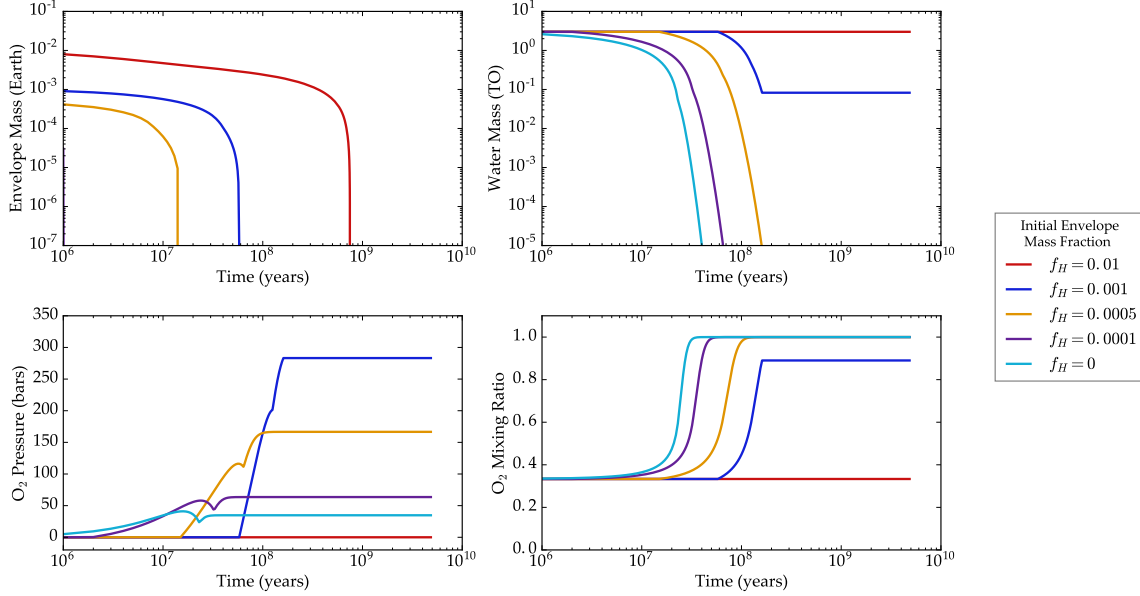
Fig. 13.— Evolution of the water and O_2 contents assuming Proxima b formed with a hydrogen envelope and 3 TO. Line colors correspond to different initial envelope mass fractions f_H, ranging from 0.0001 to 0.01. In all cases, the envelope evaporates completely prior to 1 Gyr. For $f_H \lesssim 0.001$, the H envelope evaporates quickly enough to allow complete desiccation of the planet prior to its arrival in the HZ at $\sim$ 160 Myr (note the purpleline on the y-axis in the top left panel). For $f_H \approx 0.01$, the envelope evaporates a few hundred Myr *after* the planet enters the HZ, preventing any water from being lost and O_2 from accumulating in the atmosphere. This is the most favorable scenario for a potentially habitable Proxima b.
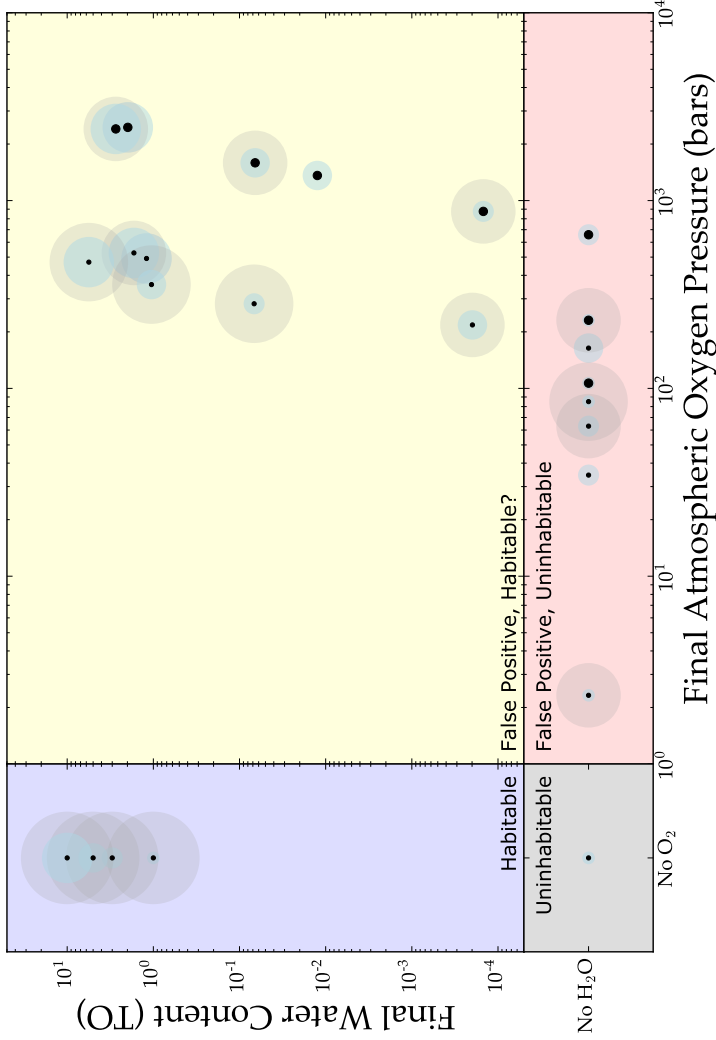
Fig. 14.— Multiple evolutionary pathways for the water on Proxima b. These plots show the final water and final atmospheric O$_2$ content of the planet for a suite of different initial conditions, assuming inefficient surface sinks for O$_2$. Different marker styles indicate different values of the planet mass, the initial water content, and the initial hydrogen envelope mass fraction f_H (the final value of f_H is zero for all planets shown here). Each panel is divided into quadrants, corresponding to planets that at the end of the simulation have water but no O$_2$ (top left, blue), water and O$_2$ (top right, yellow), neither water nor O$_2$ (bottom left, gray), and O$_2$ but no water (bottom right, red). Habitable planets are those in region shaded blue. Planets in the grey region are desiccated and therefore uninhabitable. Planets in the red region are likewise uninhabitable, but may have atmospheric O$_2$, which could be incorrectly attributed to biology. Finally, planets in the yellow region are habitable, since they have abundant surface water, but may also have substantial atmospheric O$_2$, which could be an impediment to atmospheric characterization, as the presence of water and O$_2$ could fool observers into believing they are inhabited.
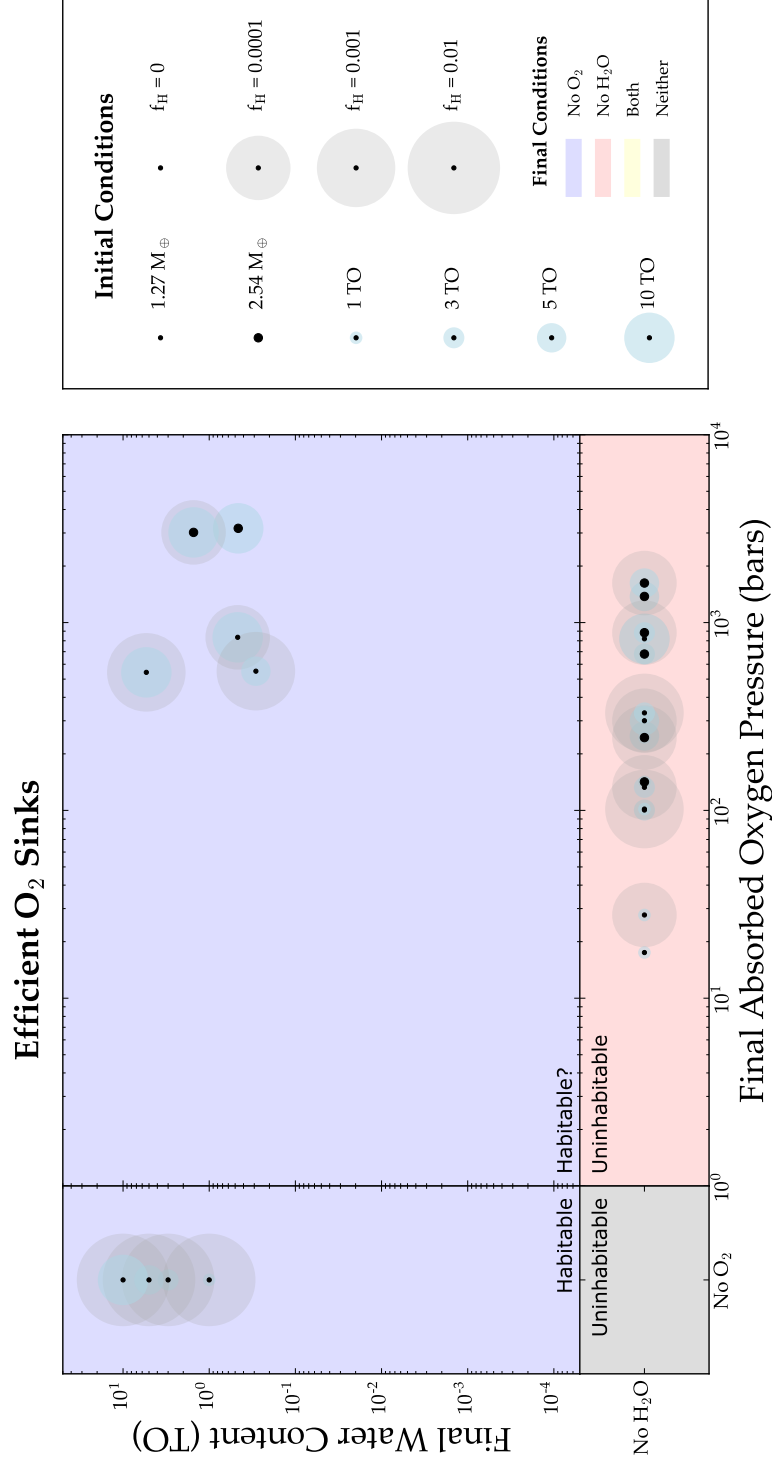
Fig. 15.— Same as Fig. 15, but assuming Proxima b has efficient O_2 sinks, preventing the buildup of significant oxygen in the atmosphere. The x axis now shows the total amount of oxygen absorbed at the surface.

which Proxima b formed with a hydrogen envelope of mass $\sim 0.01\,\mathrm{M_\oplus}$ is the most favorable for habitability, as such a planet would be a "habitable evaporated core" (Luger et al. 2015) and experience no water loss. However, if Proxima b is more massive than $1.27\,\mathrm{M_\oplus}$, the envelope may not completely evaporate and the planet may not be habitable today. Second, scenarios in which Proxima b formed with less hydrogen can still result in present-day surface water, but in all cases in which water remains, $\gtrsim 200$ bars of oxygen are retained. Finally, the primary effect of a larger planet mass is to increase the amount of oxygen in the atmosphere and/or absorbed at the surface; while in some cases a larger planet mass can result in less water loss, habitable scenarios are more likely for a lower planet mass, consistent with the results of Luger & Barnes (2015).

Further data on Proxima b will greatly aid in distinguishing between these multiple evolutionary pathways. In particular, constraints on the exact mass (via measurements of the orbital inclination) could inform the atmospheric escape history, while a value for the radius could provide a handle on whether or not a hydrogen envelope is present.

4.5. Internal Evolution

4.5.1. Role of Radiogenic Abundances

Modeling the internal evolution of Proxima b is challenging due to the large number of unknowns about its composition, structure, thermal state, atmosphere, and the evolution of its environment, *e.g.* flares stripping the atmosphere. In this section we first consider how different abundances of radiogenic isotopes could affect its evolution, then we consider tidal heating.

As described in § 3.6 we consider four possible abundance patterns for Proxima b: Earth-like, chondritic, 1 ppt ^{26}Al, and inert (no radioactivity). In all cases we begin with a core temperature of 6000 K and a mantle temperature of 3000 K, except for the chondritic case in which the latter is 4000 K. This change was necessary to avoid numerical issues associated with the high radiogenic power.

In Fig. 16 we show the evolution of the radiogenic power, mantle temperature, inner core radius, magnetic moment, magnetopause radius and surface energy flux for the four cases. The dashed black lines represent the modern Earth's value.

In the top left panel we show the evolution of the total radiogenic power produced in the core, mantle and surface. Initially, the power from ^{26}Al is over 2×10^{18} W, but with a half-life of 700,000 years, its contribution to the energy budget drops to 0 within 10^7 years.
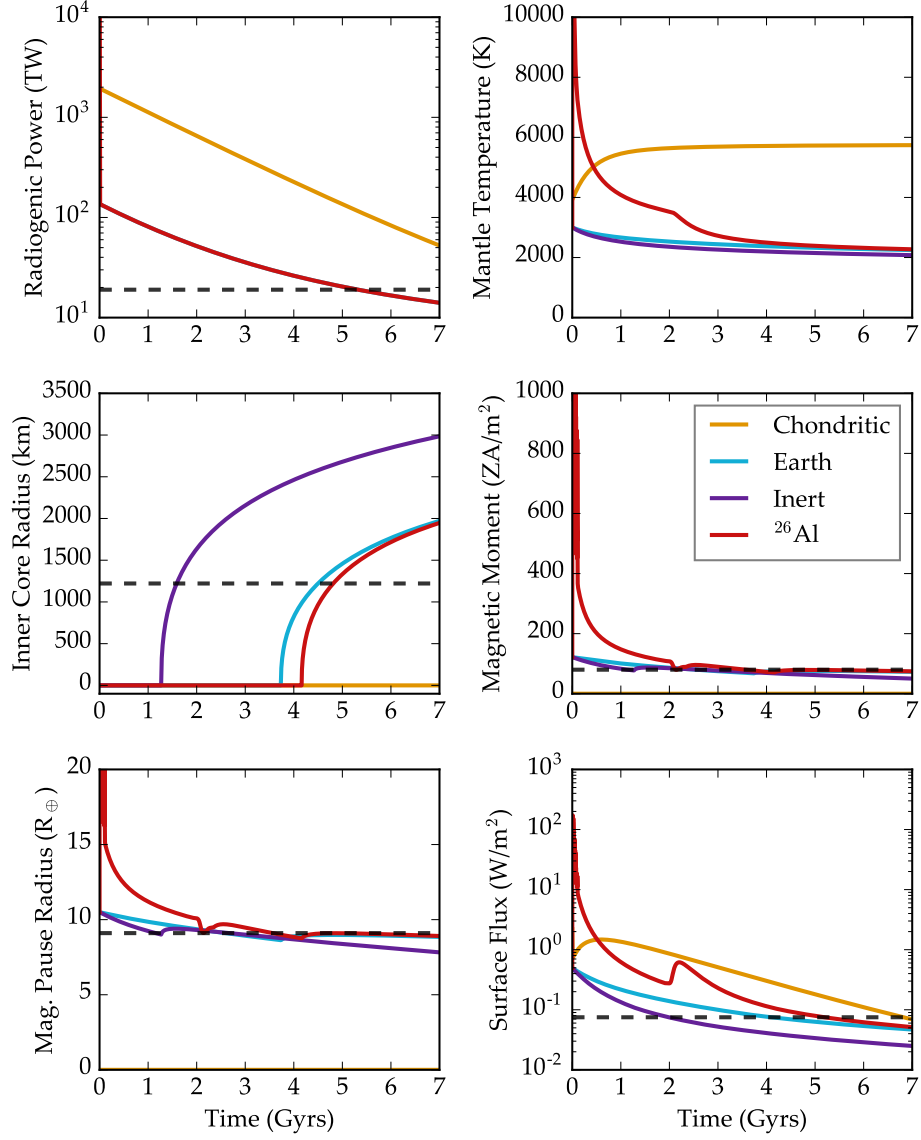
Fig. 16.— Evolution of internal properties of planet b for different assumptions of radiogenic inventory: Earth-like in blue, chondritic in orange, 1 part per trillion ^{26}Al in red, and inert in purple. Values for the modern Earth are shown with the dashed black line. *Top left:* Radiogenic power. The Earth curve is behind the ^{26}Al curve except for time = 0. *Top right:* Mantle Temperature. In the chondritic case (orange), the mantle heats to about 5500 K, where it remains for the next 6 Gyr. For the ^{26}Al (red) case, the kink at 2 Gyr is due to latent heat released as the mantle begins to solidify. *Middle left*: Size of the solid inner core. *Middle right*: Magnetic moment. The chondritic case has a non-convecting core and no dynamo. *Bottom left:* Magnetopause radius assuming the solar wind pressure at Proxima b is 0.2 times that at Earth. *Bottom right:* Surface energy flux. The hump at 2 Gyr for the ^{26}Al case is due to mantle solidification.

The Earth-like case is hidden behind the ^{26}Al curve except at $t = 0$.

The mantle temperature is shown in the top right panel. The Earth and inert cases are similar, but, as expected, the inert case temperature drops more quickly with no radiogenic power in the interior. The enriched cases show interesting features as the energy transport mechanisms change. The chondritic case heats to about 5500 K due to the large radiogenic heat production. The ^{26}Al mantle solidifies at about 2 Gyr producing the kink as latent heat is released.

The case with ^{26}Al is particularly interesting because it predicts initial mantle temperatures in excess of 10^4 K, which is clearly unphysical. While part of the implausible behavior is due to the "cold" initial mantle temperature of 3000 K, the real issue is that the heating from just 1 ppt of ^{26}Al is so large that we should expect the silicate mantle to begin to vaporize, which we do not model. However, we do see that after this initial burst of heating, the planet settles into an Earth-like evolution. Thus, if heating from ^{26}Al is just a passing energy source, it may not affect the evolution. On the other hand, the heating could be so large that the planet may be irrevocably altered. At this time, we merely point out that the influence of ^{26}Al could be significant for planets with formation times of order 1 Myr, which is similar to ^{26}Al's half-life.

In the middle left panel, we show the size of the inner core. The inert case produces the earliest inner core, though the entire core (which has a radius of 3400 km) does not solidify. The burst of ^{26}Al heating causes a slight delay in inner core formation compared to Earth, while the chondritic case does not experience any core solidification, even after 7 Gyr.

The middle right panel shows the evolution of the magnetic moment for the four different cases. The inert and Earth cases are very similar, but the other two are very different. The ^{26}Al case has a very strong magnetic field early on, but it decays rapidly after this power source is depleted. The chondritic case has no magnetic field because the core cooling rate is insufficient to drive convection in the core.

The bottom left panel shows the magnetopause radius for Proxima assuming a stellar wind pressure that is 20% weaker than the the Earth experiences. This value is an upper limit (Wood et al. 2001), so our values here are conservative — the actual stand-off radius could be larger — except for the chondritic case, for which there is no magnetic field.

Finally, the bottom right panel shows the surface energy flux for each case. Not surprisingly the chondritic case maintains the highest heat fluxes, near 1 W/m^2, which is similar to Io's value of 2.5 W/m^2 (Veeder et al. 1994). The humps and kinks are due to the changing heat sources described above. The ^{26}Al case begins with a very large heat flux, in the range of 100 W/m^2, which is nearing the value to trigger a runaway greenhouse. The inert case

emits less energy than Earth. Note that this lower energy flux partially explains the similarity in the mantle temperatures with time; the Earth case produces and loses more energy than the inert case.

4.5.2. Evolution with Tidal Heating

Next, we examine the role of tidal heating on the evolution of the planet's interior and orbit. Rather than also include the different radiogenic abundances described above, we consider the "Earth" case but with three initial eccentricities: 0.05, 0.1 and 0.2. In Fig. 17 we show the evolution of 9 quantities as a function of time for the three initial eccentricities.

The thermal evolution of the planet changes significantly because the tidal power can be in excess of 100 TW, or twice the total power of the modern Earth. As discussed in Driscoll & Barnes (2015), we find that the planet's tidal response evolves with the thermal state of the interior, preventing the unrealistically large tidal power predicted by simpler equilibrium tide models; see above. Essentially, tidal heating increases mantle temperature, lowering mantle viscosity, which raises the tidal Q. In fact, Proxima b may be close to a "steady-state" regime as defined in Driscoll & Barnes (2015), where the surface heat flow balances tidal dissipation in the mantle so that planet cools very slowly. This steady-state relies on the negative feedback between mantle temperature and tidal dissipation and the positive feedback between temperature and heat flow, so that a decrease in temperature causes increased tidal heating, pushing the temperature back up.

The mantle cooling rate is more sensitive to tidal dissipation than the core because dissipation in the model occurs only in the mantle. The core cooling rate does change somewhat with tidal dissipation, but its effect on the magnetic moment is muted because the magnetic moment depends on core convective heat flux to the 1/3 power. Note, however, that the inner core grows earlier and more rapidly than in the Earth case of Fig. 16 because the core is cooling more rapidly. This counterintuitive effect of high tidal heating rates causing rapid cooling and early core nucleation was also found by Driscoll & Barnes (2015). Although none of our cases achieve a fully solid core, which would quench the dynamo, they are close, and given the uncertainty in both the composition and structure of Proxima b, it is possible that the core has already solidified, preventing a core dynamo, and exposing the atmosphere to stellar flares.
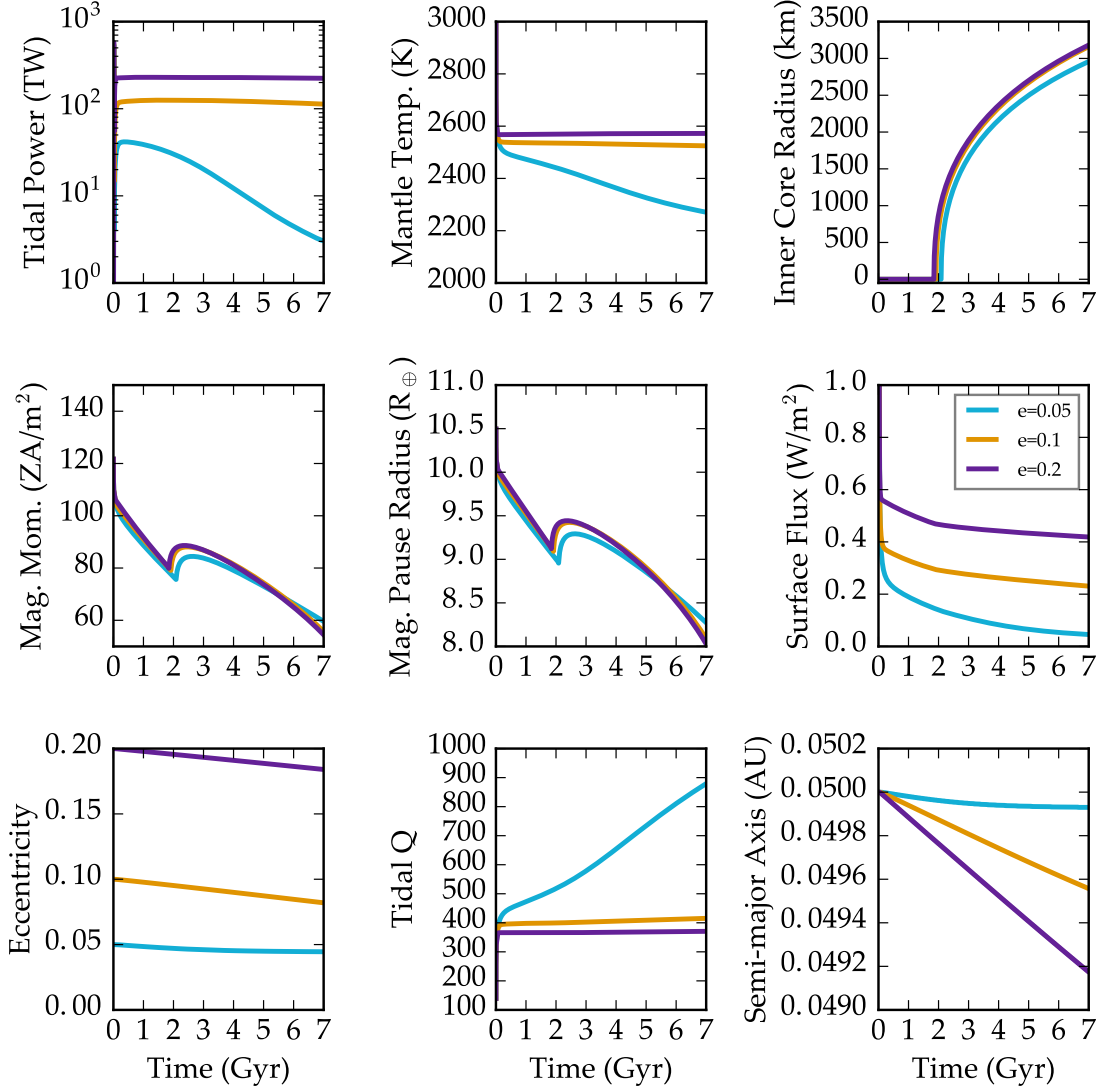
Fig. 17.— Evolution of internal properties of planet b for three different initial eccentricities, as shown in the legend, and assuming the Earth-like levels of radiogenic isotopes. *Top left:* Power generated by tidal heating. *Top middle:* Mantle temperature. *Top right:* Radius of the inner core. *Middle left:* Magnetic moment. *Middle:* Magnetopause radius. *Middle right:* Surface energy flux. *Bottom left:* Orbital eccentricity. *Bottom middle:* Tidal Q. *Bottom right:* Semi-major axis.

4.6.   Habitable Evaporated Core Scenarios

Since a possible path towards habitability for Proxima b is the "habitable evaporated core" scenario of Luger et al. (2015), we seek to model how the presence of an evaporating hydrogen envelope and surface oceans impact the tidal and orbital evolution of Proxima b. To do so, we couple the atmospheric escape physics of ATMESC, tidal evolution using EQTIDE, the Earth-calibrated geophysical interior models of RADHEAT and THERMINT and the stellar evolution of STELLAR.

We model the combined tidal contributions of the envelope, oceans, and solid interior via the following relation for the body's total tidal Q:

$$-Im(k_2) = -Im(k_2)_{interior} + \frac{k_{2_{ocean}}}{Q_{ocean}} + \frac{k_{2_{envelope}}}{Q_{envelope}}, \qquad (10)$$

where $Im(k_2)$ is the imaginary part of the Love number (see Driscoll & Barnes 2015). In Eq. (10) we remove terms if there is no component to contribute to Proxima b's net tidal interaction, $i.e.$ no ocean or no envelope.

In the general case when a hydrogen envelope is present, we only consider the coupled tidal effects of the interior and the envelope as any water is likely to be supercritical due to the high pressure exerted by the envelope. When an envelope is not present, we consider the tidal contribution of surface oceans only if the planet is not in the runaway greenhouse limit since otherwise all water would be present in the atmosphere.

We simulate four cases that bracket the potential past tidal evolution of Proxima b. The first case, "CPL," assumes a constant tidal $Q = 12$ analogous to the simulations described in § 4.2 and consistent with observations of Earth today (Dickey et al. 1994; Williams et al. 1978; Yoder 1995). This low tidal Q is due to efficient energy dissipation by oceans. The "No Ocean" case assumes the tidal interaction is dominated by the planet's interior as determined by RADHEAT and THERMINT, while the "Ocean" case generalizes the "No Ocean" case by assuming Proxima b had an initial inventory of 10 ETO of water with $Q_{ocean} = 12$. The full habitable evaporated core "Envelope" case considers a planet with a hydrogen envelope that has an initial mass fraction of 0.001 of the planet's total mass with $Q_{envelope} = 10^4$, which is consistent with measurements of Neptune's tidal Q (Zhang & Hamilton 2008). The "Envelope" case starts with 4.5 TO to demonstrate the envelope's ability to shield surface water from atmospheric escape. We set $k_{2_{ocean}} = 0.3$ and $k_{2_{envelope}} = 0.01$ to let the thermal interior and oceans determine k_2 as these components dominate both the size and mass of the planet. The results of the simulations are shown in Figure 18.

The "No Ocean" case, dominated by the mantle, reaches tidal a Q of a few 100 and undergoes minimal tidally-driven orbital evolution until after about 1 Gyr. Initially, the
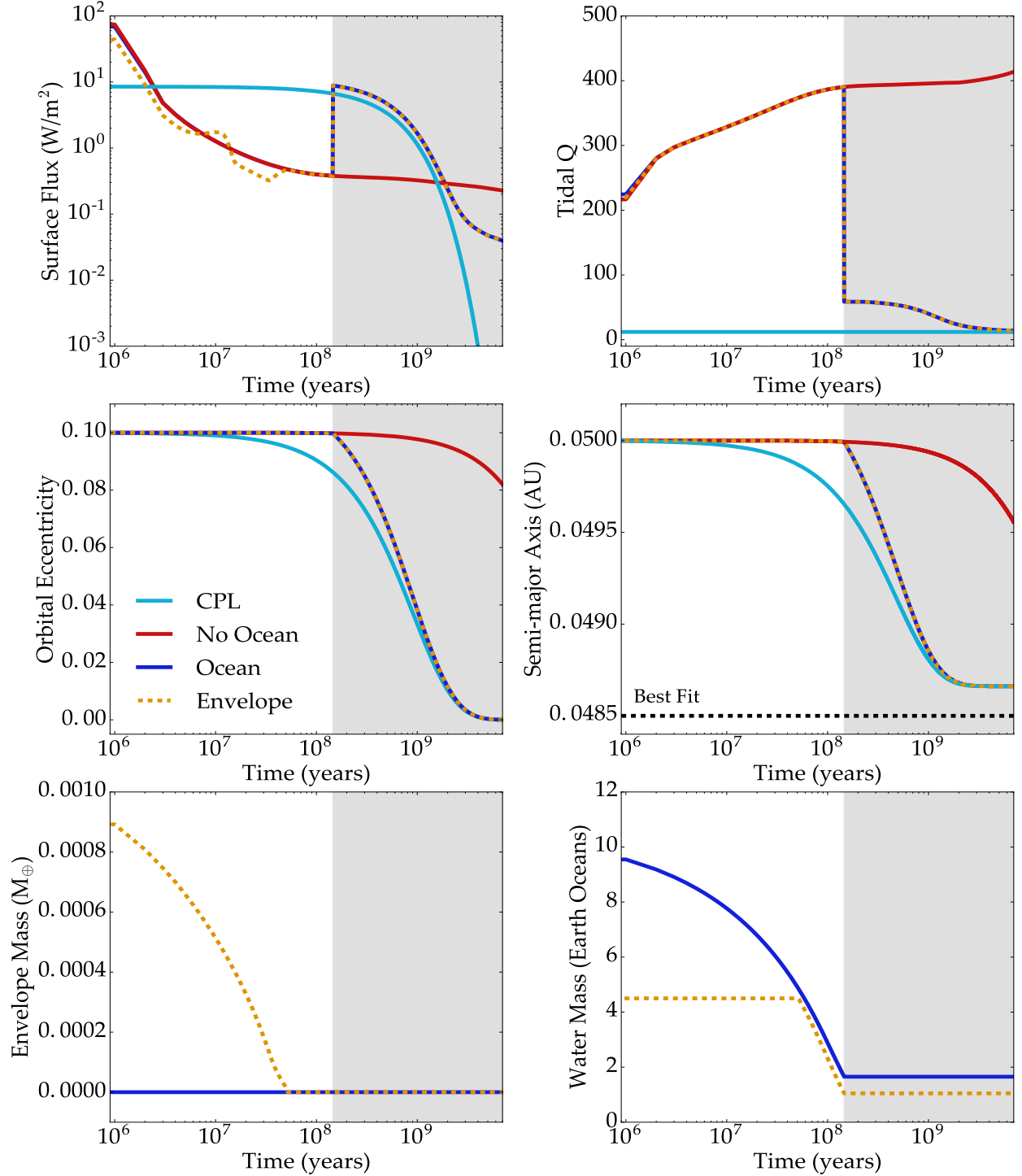
Fig. 18.— Evolution of the orbital, tidal and atmospheric properties of Proxima b for the "CPL" case in light blue, "No Ocean" case in red, "Ocean" case in dark blue, and the "Envelope" case in orange with the dashed line for clarity. The grey shaded region indicates when the planet is in the HZ. *Top left:* Surface Flux. *Top right:* Tidal Q. *Middle left:* Orbital Eccentricity. *Middle right:* Semi-major Axis. *Bottom left:* Envelope Mass. *Bottom right:* Surface Water Mass.

bulk of the surface flux stems from rotational tidal energy dissipation which lessens as the planet approaches a tidally locked state at around 15 Myr. Early on in the "Ocean" case, the planet is in a runaway greenhouse phase in which all the water is locked up in the atmosphere and subject to escape of hydrogen and oxygen from photolysis, decreasing the water mass. Its tidal evolution mirrors the "No Ocean" case as the mantle dominates. Once the star's luminosity decreases enough, the planet enters the HZ at around 10^8 years and the remaining water condenses to the surface. The presence of surface oceans dramatically decreases the tidal Q leading to rapid orbital circularization and a substantial surface flux increase via tidal energy dissipation. We note that the tidal Q of the surface oceans may depend on the total ocean mass and the presence of shallow seas, which should be explored in future studies.

The "Envelope" case has a slightly different surface flux and tidal Q than the Ocean and No Ocean cases as the envelope contributes minimally to the initial tidal evolution and the planet's radius evolves with time. Stellar UV flux completely strips the hydrogen envelope after about 4×10^7 years, causing the mantle to again dictate the tidal interaction. The hydrogen envelope initially shields the planet's water allowing for enough to survive subsequent photolysis. About 1 TO of the initial 4.5 remain once the planet enters the HZ if we assume the planet has inefficient oxygen sinks. With the envelope gone, surface water dominates the tides and its evolution mirrors that of the "Ocean" case.

5. Discussion

In the previous section we outlined numerous possibilities for the history of Proxima b. We considered processes spanning the planet's core to the Milky Way galaxy and find that effects at all these scales could be important in the history of our closest exoplanet. In this section, we summarize the results in terms of the potential atmospheres that Proxima b might have, which are considered in detail in (Meadows et al., in prep.). Then we examine the likelihood that it is currently habitable.

5.1. Atmospheric States

5.1.1. Earth-Like

We find that some scenarios allow for the planet to currently support liquid surface water. In particular, the "habitable evaporated core" scenario (Luger et al. 2015) is particularly promising as it can avoid both the high-luminosity pre-main sequence (pre-MS) phase

and any devastating tidal heating that may occur while the planet "surfs" the HZ migration, or during circularization after orbital destabilization. Such a world may be enriched in deuterium that remained during hydrogen escape, and it may also be geothermally active if it is young and enriched in potassium.

Another possibility is that Proxima b formed at a larger orbital distance and was scattered in to its current location by a system-wide instability, which may have been triggered by a close passage with α Cen A and B, see § 4.1. If the instability happened after the star reached the main sequence, then the planet would have arrived in the HZ after its position had stabilized. If b's eccentricity after the instability was larger than about 0.35, then there is some danger that tidal heating could have triggered a runaway greenhouse (see Fig. 7), but it may have been short-lived enough to permit habitability.

Another low-probability possibility is that even if the planet became desiccated during the pre-MS phase, impact from water-rich bodies could simultaneously blow off the CO_2 and/or O_2 atmosphere while delivering water. This scenario would require a specific set of events to occur, but we note that close passages between Proxima and α Cen A and B could destabilize any putative "exo-Oort Clouds" that could have existed around the stars. Current numerical models do not permit a robust calculation of this possibility, so it remains a viable path for Proxima b to be habitable.

Although these atmospheric states permit habitability, we must bear in mind that the rotation period is either synchronous or in a spin-orbit resonance due to tidal effects (Rodríguez et al. 2012). The rotation rate is therefore longer than on Earth and so atmospheric dynamics would be different. If synchronous, it is likely that the planet's daylit side is covered in clouds (Yang et al. 2013).

The obliquity of Proxima b is likely small, even in a Cassini state from the influence of companion planets, due to tidal damping. Thus, we do not expect the obliquity to significantly impact the climate in the form of seasons or heat transport. Ultimately, this is one way in which Proxima b's climate will be different from Earth.

5.1.2. Habitable, but Dry

As shown in Fig. 11, a dry planet would enter a potentially habitable state earlier than an Earth-like planet, and hence it may be that Proxima b is a habitable world, but with little liquid water. This could occur if the planet formed *in situ* and the gas disk was able to shield the planet from water loss. The habitable evaporated core scenario is also a possibility if the core was dry and a thin layer of hydrogen could be blown away. On the other hand,

a planet without much water does not need to spend much time in a runaway greenhouse to become desiccated. For this latter reason, we conclude the dry and habitable case to be unlikely, but our models cannot exclude it.

5.1.3. Venus-Like

Regardless of whether Proxima b spent significant time in a runaway greenhouse prior to the arrival of the HZ, it could be in a runaway greenhouse state like Venus. If it formed *in situ*, then this possibility is more likely because its first ∼100 Myr were spent interior to the HZ and hence it may have developed a dense CO_2 atmosphere as has occurred on Venus. In this case, the planet is uninhabitable as the surface temperature is too hot for liquid water, and the higher surface temperature results from greenhouse warming by CO_2.

Even if the planet avoided desiccation during the pre-MS stage, it is reasonable to assume that a Venus-like atmosphere is possible. CO_2 is a very abundant molecule in planetary atmospheres, and given its strong ability to heat the surface, high molecular weight, and strong chemical bonds, it may be able to accumulate in the HZ to large enough levels to trigger the runaway greenhouse, assuming large enough reservoirs exist.

A final possibility, mentioned above, is that past tidal heating drove the planet into a runaway greenhouse (Barnes et al. 2013). If the planet was ever in a high eccentricity state ($e > 0.35$) then the surface energy flux from the interior could have reached the critical limit of ∼300 W/m^2 (Kasting et al. 1993; Abe 1993; Goldblatt 2015). Such high surface fluxes may be short-lived if the heating can only come from the ocean (Driscoll & Barnes 2015).

5.1.4. Neptune-Like

Proxima b may have formed with sufficient hydrogen that some has been retained despite all the high energy processes that can remove it. This possibility is especially likely if it formed beyond the snow line and migrated in. Similarly to Owen & Mohanty (2016), we find that if Proxima b formed with $\gtrsim 1\%$ of its mass in the form of a hydrogen envelope, it could still possesses some hydrogen, in which case the surface may be too hot and/or the surface pressure is too high for habitability. Future measurements of Proxima b's radius can inform its present-day composition and thus settle this issue.

5.1.5. Abiotic Oxygen Atmosphere

If Proxima b formed with one or more terrestrial oceans (TO) of water, photolysis followed by hydrogen escape during the stellar pre-MS phase could have led to the buildup of substantial O_2 in the atmosphere. Although oxygen is highly reactive, thousands of bars of oxygen can be liberated through this mechanism (Luger & Barnes 2015) and hence all sinks for it may become saturated (Schaefer et al. 2016). In principle, thousands of bars of oxygen could remain in the atmosphere, but this figure is most likely lower, as much of the oxygen will be consumed in the process of oxidizing the surface. In this case Proxima b may be uninhabitable, given that little free energy may be available at the surface for early organisms to take a hold. Life on Earth is thought to have emerged in an extremely reducing environment (Oparin 1924; Haldane 1929), with access to high energy gradients to fuel early metabolisms; such a reducing environment may not be present on Proxima b.

In many of the scenarios in which Proxima b develops an O_2-rich atmosphere, it also maintains at least some of its initial water. After the end of the Pre-MS phase, the O_2, H_2O and CO_2 greenhouse warming could be sufficient to prevent water from accumulating on the surface, and hence it could have significant abundance in the stratosphere. While the simultaneous detection of water and oxygen has traditionally been envisaged as an ideal combination for life detection (Des Marais et al. 2002), in the case of Proxima b, it is insufficient to prove habitable conditions exist, let alone that life is present.

Alternatively, if the greenhouse gases are at low enough levels in the atmosphere, then it may be possible for liquid water to accumulate on the planetary surface and this planet would meet the traditional definition of "habitable." However, as argued above, such a planet would likely be incapable of supporting life. Thus, the detection of atmospheric oxygen as well as the presence of surface liquid by other means, *e.g.* glint (Robinson et al. 2010), would not be sufficient evidence that the planet is habitable.

5.1.6. Water and Oxygen, but Uninhabitable?

Figs. 12—15 show an interesting possibility in which large amounts of oxygen are built up by the pre-MS runaway, butnot all the water is destroyed. If this occurs, water and oxygen may both be present in the atmosphere, but the large O_2 inventories may prevent the development of Earth-like biomolecules. Thus, the simultaneous detection of water and O_2 in Proxima b's atmosphere is not necessarily a biosignature, or really even habitability in the sense that life could originate.

5.1.7. No Atmosphere

Since Proxima b is subjected to repeated flaring events and other activity (Walker 1981; Davenport 2016), it may be that the atmosphere has been permanently destroyed. Such a process is difficult to envision, as it would require all the volatiles in the mantle to have been degassed and blown away. However, if the planet was tidally heated for a long time, mantle convection may have been vigorous and perhaps total volatile depletion is possible, especially if the planet is of order 7 Gyr old and if the core has solidified, quenching the magnetic dynamo (Driscoll & Barnes 2015). Another possibility is that a recent stellar eruption has temporarily stripped away the atmosphere, which will reform by outgassing.

5.2.   Is Proxima b Habitable?

Planetary habitability is a complicated feature to model quantitatively and Proxima b is no exception. We do know that the planet has sufficient energy to support life, assuredly has enough bioessential elements, and is old enough for life to have gained a foothold, assuming Earth isn't an extreme outlier. The biggest questions are if it is terrestrial, and if it possesses vast reservoirs of liquid water. At this time, it is impossible to determine the probability that it does support liquid water, so we cannot answer the eponymous question. As always, more data are needed.

However, our analysis does provide some important information on where to focus future efforts. As liquid water is vital, it is paramount to determine the pathways that allow the planet to have accreted and retained the water. However, even if the planet forms with water, our investigations have shown that it will not necessarily be retained. If it formed *in situ* or arrived in the HZ at the time of the dispersal of the gas disk, then Proxima b had to endure ~ 150 Myr in a runaway greenhouse state; see § 4.3 and Luger & Barnes (2015).

Even if the planet arrived in its orbit late, perhaps following an orbital instability, the water may have to survive a "tidal greenhouse" in which tidal heating drives water loss, see § 4.5 and Barnes et al. (2013). Such high tidal heating rates may require very large eccentricity and/or abnormally low Q values, but the former is certainly possible during planet-planet scattering events (Chatterjee et al. 2008), or perhaps by Kozai-like oscillation driven by perturbations from the α Cen A and B pair if the orbit of Proxima Centauri was much smaller in the past (Desidera & Barbieri 2007). If an additional planet in the system is massive, on an eccentric orbit, and/or on a highly inclined orbit, then it, too, may induce perturbations that maintain eccentricities (Takeda & Rasio 2005), possibly in the range of a tidal greenhouse. A planet in a Cassini state may receive additional tidal heating, further

increasing the risk of a tidal greenhouse. As shown in § 4.5, the eccentricity of b will damp, but the timescale can be very long. Large eccentricities are not well-modeled by equilibrium tide theory, even with a proper accounting of geophysical features as in the THERMINT module, so it is difficult at present to assess the role of tidal heating in water retention.

Another possible route to water loss is through temporary or permanent atmosphere erosion by flares and coronal mass ejections. It is possible that these events could blast away the atmosphere completely, in which case liquid water on the surface is not stable. Should the atmosphere reform, the water may return to the liquid state, but it is certainly plausible that some events are powerful enough to remove the water in one event, or, more likely, repeated bombardments would slowly remove the atmosphere (Cohen et al. 2015). Our analysis doesn't provide a direct measurement of this phenomenon, but we note that some geophysical models for the planet predict high heating rates in the mantle will suppress core convection. In those cases, the magnetic field is quenched and is not capable of deflecting charged particles. Even if the planet does have a magnetic field, Vidotto et al. (2013) find that planets around typical M dwarfs may have their magnetopause distances driven to the planet surface by the star's magnetic field. However, it is not clear that a magnetic field is always beneficial for life, as it also increases the cross-sectional area of the planet for charged particles and funnels the energy into the magnetic poles, possibly increasing mass loss.

These processes are all clear dangers for the habitability of Proxima b. Yet, we are also able to identify pathways that produce decidedly Earth-like versions of planet b. As shown in Fig. 18, if the planet formed with 0.1% of its mass in a hydrogen envelope, 4.5 Earth oceans of water, then the combined effects of the stellar evolution, envelope evolution and atmospheric escape, tidal evolution, and geophysical evolution predict a planet with 1 Earth ocean of surface water, no hydrogen envelope, and a semi-major axis within the observed uncertainties. A planet like this could evolve similarly to Earth, and therefore may have Earth-like conditions today.

A final possibility is that Proxima b, receiving only 65% of Earth's insolation, may have an ice-covered surface, but with a liquid water mantle, similar to Europa. For such a planet, the water is heated by the energy from accretion, radiogenic sources and/or tidal heating. Ice is much more absorptive at the longer wavelengths of light that Proxima emits and so it may be difficult to ice over the planet (Joshi & Haberle 2012; Shields et al. 2013), especially since it probably spent hundreds of Myr in a runaway greenhouse. But if a reflective haze and/or cloud layer could form, it could reflect away the light before it reaches the surface (*e.g.* Arney 2016). This possibility seems unlikely, but we cannot rule out that the planet is a "super-Europa" (Barnes & Heller 2013), a scaled up version of the icy satellites of our Solar System and with a potentially inhabited subsurface water layer.

Proxima b may or may not be habitable. While we are only able to identify a narrow range of pathways that permit habitability, we must bear in mind that our model, while including phenomena over sizescales of meters to kpc, is simple and does not include many potential feedbacks. The geochemistry of exoplanets is a gaping hole in scientific knowledge, and one can easily imagine how other systems may maintain liquid water with geochemical cycles not present in our Solar System. Similarly, liquid surface water may represent a sort of "planetary attractor," in which planets in the HZ naturally and typically evolve toward a state in which their surfaces support liquid water.

6. Conclusions

We have performed a detailed analysis of the evolution of the Alpha Centauri triple star system with a specific focus on Proxima Centauri b's habitability. We find that many disparate factors are important, including the stellar system's orbit in the galaxy (§ 4.1), the orbital and rotational evolution of the planets (§ 4.2), the stellar evolution (§ 4.3), the geophysical evolution (§ 4.5), and the atmospheric evolution (§ 4.4). We find that many evolutionary pathways are permitted by the data and hence the planet may currently exist in one of many possible states.

We conclude that Proxima b may be habitable, but identify the retention of water as the biggest obstacle for Proxima b to support life. Water loss may occur through multiple channels operating in tandem or in isolation, including desiccation during the Pre-MS, excessive tidal heating, or atmospheric destruction by flares and coronal mass ejections. We find the most likely pathway for habitability is if planet b formed with a thin hydrogen envelope of order 10^{-2} $M_\oplus$ which was eroded by the early XUV evolution of the host star; see § 4.3 and Luger et al. (2015). In that case, Proxima b is a "habitable evaporated core" and has followed a very different trajectory than Earth did on their paths to liquid surface water.

Regardless of Proxima's habitability, it offers scientists an unprecedented window into the nature of terrestrial planets. At only 1.3 pc distance, we will be able to study this planet in detail with future missions, should they be designed appropriately; see Meadows (et al., in prep.). If Proxima b is uninhabitable, we may be able to determine how that happened and how Earth avoided the same fate. At a minimum, the discovery of Proxima Centauri b has ushered in a new era in comparative planetology, or perhaps it is the first step in the discovery of extraterrestrial life.

REFERENCES

Abe, Y. 1993, Lithos, 30, 223

Abe, Y., Abe-Ouchi, A., Sleep, N. H., & Zahnle, K. J. 2011, Astrobiology, 11, 443

Aksnes, K., & Franklin, F. A. 2001, AJ, 122, 2734

Allen, C., & Herrera, M. A. 1998, Rev. Mexicana Astron. Astrofis., 34, 37

Allende Prieto, C., Barklem, P. S., Lambert, D. L., & Cunha, K. 2004, A&A, 420, 183

Anders, E., & Grevesse, N. 1989, Geochim. Cosmochim. Acta, 53, 197

Anglada-Escudé, G. 2016, Nature

Anosova, J., Orlov, V. V., & Pavlova, N. A. 1994, A&A, 292, 115

Araki, T., Enomoto, S., Furuno, K., et al. 2005, Nature, 436, 499

Arevalo, R., McDonough, W. F., & Luong, M. 2009, Earth and Planetary Science Letters, 278, 361

Armstrong, J. C., Barnes, R., Domagal-Goldman, S., et al. 2014, Astrobiology, 14, 277

Arney, G. 2016, AsBio

Atobe, K., & Ida, S. 2007, Icarus, 188, 1

Baraffe, I., Chabrier, G., Allard, F., & Hauschildt, P. H. 1998, A&A, 337, 403

Baraffe, I., Homeier, D., Allard, F., & Chabrier, G. 2015, A&A, 577, A42

Barnes, J. R., Jenkins, J. S., Jones, H. R. A., et al. 2014, MNRAS, 439, 3094

Barnes, R. 2016, CeMDA

Barnes, R., Greenberg, R., Quinn, T. R., McArthur, B. E., & Benedict, G. F. 2011, ApJ, 726, 71

Barnes, R., & Heller, R. 2013, Astrobiology, 13, 279

Barnes, R., Mullins, K., Goldblatt, C., et al. 2013, Astrobiology, 13, 225

Barnes, R., Raymond, S. N., Jackson, B., & Greenberg, R. 2008, Astrobiology, 8, 557

Bazot, M., Christensen-Dalsgaard, J., Gizon, L., & Benomar, O. 2016, MNRAS, 460, 1254

Benedict, G. F., Nelan, E., McArthur, B., et al. 1993, PASP, 105, 487

Benedict, G. F., McArthur, B., Nelan, E., et al. 1998, AJ, 116, 429

Berger, A., & Loutre, M. F. 1991, Quaternary Science Reviews, 10, 297

Bouchy, F., & Carrier, F. 2001, A&A, 374, L5

—. 2002, A&A, 390, 205

Boyajian, T. S., von Braun, K., van Belle, G., et al. 2012, ApJ, 757, 112

Brasser, R., Ida, S., & Kokubo, E. 2014, MNRAS, 440, 3685

Carrier, F., & Bourban, G. 2003, A&A, 406, L23

Carter-Bond, J. C., O'Brien, D. P., & Raymond, S. N. 2012, ApJ, 760, 44

Chaplin, W. J., Basu, S., Huber, D., et al. 2014, ApJS, 210, 1

Chatterjee, S., Ford, E. B., Matsumura, S., & Rasio, F. A. 2008, ApJ, 686, 580

Ciesla, F. J., Mulders, G. D., Pascucci, I., & Apai, D. 2015, ApJ, 804, 9

Cincunegui, C., Díaz, R. F., & Mauas, P. J. D. 2007, A&A, 461, 1107

Cohen, O., Drake, J. J., Glocer, A., et al. 2014, ApJ, 790, 57

Cohen, O., Ma, Y., Drake, J. J., et al. 2015, ApJ, 806, 41

Colombo, G. 1966, AJ, 71, 891

Correia, A. C. M., Levrard, B., & Laskar, J. 2008, A&A, 488, L63

Darwin, G. H. 1880, Royal Society of London Philosophical Transactions Series I, 171, 713

Davenport, J. 2016, ApJ

Delfosse, X., Forveille, T., Ségransan, D., et al. 2000, A&A, 364, 217

Des Marais, D. J., Harwit, M. O., Jucks, K. W., et al. 2002, Astrobiology, 2, 153

Desidera, S., & Barbieri, M. 2007, A&A, 462, 345

Dickey, J. O., Bender, P. L., Faller, J. E., et al. 1994, Science, 265, 482

Dole, S. H. 1964, Habitable planets for man

Dotter, A., Chaboyer, B., Jevremović, D., et al. 2008, ApJS, 178, 89

Downes, J. J., Román-Zúñiga, C., Ballesteros-Paredes, J., et al. 2015, MNRAS, 450, 3490

Driscoll, P., & Bercovici, D. 2014, Physics of the Earth and Planetary Interiors, 236, 36

Driscoll, P. E., & Barnes, R. 2015, Astrobiology, 15, 739

Dye, S. T. 2010, Earth and Planetary Science Letters, 297, 1

Efroimsky, M., & Makarov, V. V. 2013, ApJ, 764, 26

Endl, M., & Kürster, M. 2008, A&A, 488, 1149

Erkaev, N. V., Kulikov, Y. N., Lammer, H., et al. 2007, A&A, 472, 329

Ferraz-Mello, S., Rodríguez, A., & Hussmann, H. 2008, Celestial Mechanics and Dynamical Astronomy, 101, 171

Ford, E. B., Kozinsky, B., & Rasio, F. A. 2000, ApJ, 535, 385

García-Sánchez, J., Weissman, P. R., Preston, R. A., et al. 2001, A&A, 379, 634

Goldblatt, C. 2015, Astrobiology, 15, 362

Goldreich, P. 1966, AJ, 71, 1

Greenberg, R. 2009, Astrophys. J., 698, L42

Haldane, J. B. S. 1929, The Rationalist Annal., 3

Hamilton, D. P., & Ward, W. R. 2004, AJ, 128, 2510

Harrington, R. S. 1968, AJ, 73, 190

Hayden, M. R., Bovy, J., Holtzman, J. A., et al. 2015, ApJ, 808, 132

Heisler, J., & Tremaine, S. 1986, Icarus, 65, 13

Heisler, J., Tremaine, S., & Alcock, C. 1987, Icarus, 70, 269

Heller, R., Jackson, B., Barnes, R., Greenberg, R., & Homeier, D. 2010, A&A, 514, A22

Heller, R., Leconte, J., & Barnes, R. 2011, Astro. & Astrophys., 528, A27+

Henning, W. G., O'Connell, R. J., & Sasselov, D. D. 2009, Astrophys. J., 707, 1000

Hernández, J., Hartmann, L., Megeath, T., et al. 2007, ApJ, 662, 1067

Hevey, P. J., & Sanders, I. S. 2006, Meteoritics & Planetary Science, 41, 95

Hinkel, N. R., & Kane, S. R. 2013, MNRAS, 432, 36

Holmberg, J., & Flynn, C. 2000, MNRAS, 313, 209

Huang, Y., Chubakov, V., Mantovani, F., Rudnick, R. L., & McDonough, W. F. 2013, Geochemistry, Geophysics, Geosystems, 14, 2003

Hunten, D. M. 1973, Journal of Atmospheric Sciences, 30, 1481

Hunten, D. M., Pepin, R. O., & Walker, J. C. G. 1987, Icarus, 69, 532

Innes, R. T. A. 1915, Circular of the Union Observatory Johannesburg, 30, 235

Jackson, B., Barnes, R., & Greenberg, R. 2008a, MNRAS, 391, 237

—. 2009, Astrophys. J., 698, 1357

Jackson, B., Greenberg, R., & Barnes, R. 2008b, Astrophys. J., 678, 1396

Johnson, J. A., & Apps, K. 2009, ApJ, 699, 933

Joshi, M. M., & Haberle, R. M. 2012, Astrobiology, 12, 3

Joshi, M. M., Haberle, R. M., & Reynolds, R. T. 1997, Icarus, 129, 450

Kaib, N. A., Raymond, S. N., & Duncan, M. 2013, Nature, 493, 381

Kasting, J. F. 1988, Icarus, 74, 472

Kasting, J. F., Whitmire, D. P., & Reynolds, R. T. 1993, Icarus, 101, 108

Kinoshita, H. 1975, SAO Special Report, 364

—. 1977, Celestial Mechanics, 15, 277

Kopparapu, R. k., Wolf, E. T., Haqq-Misra, J., et al. 2016, ApJ, 819, 84

Kopparapu, R. K., Ramirez, R., Kasting, J. F., et al. 2013, ApJ, 765, 131

Kordopatis, G., Binney, J., Gilmore, G., et al. 2015, MNRAS, 447, 3526

Korenaga, J. 2003, Geophys. Res. Lett., 30, 20

Laird, J. B. 1985, ApJ, 289, 556

Laskar, J. 1986, A&A, 157, 59

Laskar, J., Joutel, F., & Boudin, F. 1993a, A&A, 270, 522

Laskar, J., Joutel, F., & Robutel, P. 1993b, Nature, 361, 615

Lissauer, J. J. 2007, ApJ, 660, L149

Loebman, S. R., Debattista, V. P., Nidever, D. L., et al. 2016, ApJ, 818, L6

Lopez, E. D., & Fortney, J. J. 2014, ApJ, 792, 1

Lopez, E. D., Fortney, J. J., & Miller, N. 2012, ApJ, 761, 59

Luger, R., & Barnes, R. 2015, Astrobiology, 15, 119

Luger, R., Barnes, R., Lopez, E., et al. 2015, Astrobiology, 15, 57

Luhman, K. L. 2012, ARA&A, 50, 65

Lundkvist, M., Kjeldsen, H., & Silva Aguirre, V. 2014, A&A, 566, A82

Lurie, J. C., Henry, T. J., Jao, W.-C., et al. 2014, AJ, 148, 91

MacDonald, G. J. F. 1964, Reviews of Geophysics and Space Physics, 2, 467

Malmberg, D., de Angeli, F., Davies, M. B., et al. 2007, MNRAS, 378, 1207

Matthews, R., & Gilmore, G. 1993, MNRAS, 261, L5

Matvienko, A. S., & Orlov, V. V. 2014, Astrophysical Bulletin, 69, 205

Meadows, V. et al., in prep.

Minchev, I., Famaey, B., Quillen, A. C., et al. 2012, A&A, 548, A127

Mulders, G. D., Ciesla, F. J., Min, M., & Pascucci, I. 2015, ApJ, 807, 9

Murray, C. D., & Dermott, S. F. 1999, Solar system dynamics

Neuforge-Verheecke, C., & Magain, P. 1997, A&A, 328, 261

Oparin, A. 1924, The Origin of Life (Moscow), tr. in J. D. Bernal, The Origin of Life, Cleveland: World, 1967

Owen, J. E., & Mohanty, S. 2016, MNRAS, 459, 4088

Peale, S. J., Cassen, P., & Reynolds, R. T. 1979, Science, 203, 892

Pierrehumbert, R., & Gaidos, E. 2011, ApJ, 734, L13

Pierrehumbert, R. T. 2011, ApJ, 726, L8

Pourbaix, D., & Boffin, H. M. J. 2016, A&A, 586, A90

Pourbaix, D., Nidever, D., McCarthy, C., et al. 2002, A&A, 386, 280

Poveda, A., Allen, C., Herrera, M. A., Cordero, G., & Lavalley, C. 1996, A&A, 308, 55

Raghavan, R. S., Schoenert, S., Enomoto, S., et al. 1998, Physical Review Letters, 80, 635

Rauch, K. P., & Hamilton, D. P. 2002, in Bulletin of the American Astronomical Society, Vol. 34, AAS/Division of Dynamical Astronomy Meeting #33, 938

Raymond, S. N., Barnes, R., & Mandell, A. M. 2008, MNRAS, 384, 663

Raymond, S. N., Scalo, J., & Meadows, V. S. 2007, ApJ, 669, 606

Reid, I. N., Gizis, J. E., & Hawley, S. L. 2002, AJ, 124, 2721

Reiners, A., & Basri, G. 2008, A&A, 489, L45

Remy, F., & Mignard, F. 1985, Icarus, 63, 1

Ribas, I., Guinan, E. F., Güdel, M., & Audard, M. 2005, Astrophys. J., 622, 680

Rickman, H., Fouchard, M., Froeschlé, C., & Valsecchi, G. B. 2008, Celestial Mechanics and Dynamical Astronomy, 102, 111

Robinson, T. D., Meadows, V. S., & Crisp, D. 2010, ApJ, 721, L67

Rodríguez, A., Callegari, N., Michtchenko, T. A., & Hussmann, H. 2012, MNRAS, 427, 2239

Rogers, L. A. 2015, ApJ, 801, 41

Roskar, R. 2010, PhD thesis, University of Washington

Roškar, R., Debattista, V. P., Quinn, T. R., & Wadsley, J. 2012, MNRAS, 426, 2089

Sahu, K. C., Bond, H. E., Anderson, J., & Dominik, M. 2014, ApJ, 782, 89

Schaefer, L., Wordsworth, R., Berta-Thompson, Z., & Sasselov, D. 2016, ArXiv e-prints, arXiv:1607.03906

Schwieterman, E. W., Meadows, V. S., Domagal-Goldman, S. D., et al. 2016, ApJ, 819, L13

Sekiya, M., Hayashi, C., & Kanazawa, K. 1981, Progress of Theoretical Physics, 66, 1301

Sellwood, J. A., & Binney, J. J. 2002, MNRAS, 336, 785

Selsis, F., Kasting, J. F., Levrard, B., et al. 2007, Astro. & Astrophys., 476, 1373

Shapley, H. 1951, Proceedings of the National Academy of Science, 37, 15

Shields, A. L., Barnes, R., Agol, E., & Meadows, V. 2016, Astrobiology

Shields, A. L., Meadows, V. S., Bitz, C. M., et al. 2013, Astrobiology, 13, 715

Sotin, C., Grasset, O., & Mocquet, A. 2007, Icarus, 191, 337

Spada, F., Demarque, P., Kim, Y.-C., & Sills, A. 2013, ApJ, 776, 87

Storch, N. I., & Lai, D. 2014, MNRAS, 438, 1526

Takeda, G., & Rasio, F. A. 2005, ApJ, 627, 1001

Thévenin, F., Provost, J., Morel, P., et al. 2002, A&A, 392, L9

Thoul, A., Scuflaire, R., Noels, A., et al. 2003, A&A, 402, 293

Tian, F. 2015, Earth and Planetary Science Letters, 432, 126

Touma, J., & Wisdom, J. 1994, AJ, 108, 1943

Veeder, G. J., Matson, D. L., Johnson, T. V., Blaney, D. L., & Goguen, J. D. 1994, J. Geophys. Res., 99, 17095

Vidotto, A. A., Jardine, M., Morin, J., et al. 2013, A&A, 557, A67

Voûte, J. 1917, MNRAS, 77, 650

Walker, A. R. 1981, MNRAS, 195, 1029

Watson, A. J., Donahue, T. M., & Walker, J. C. G. 1981, Icarus, 48, 150

Weiss, L. M., & Marcy, G. W. 2014, ApJ, 783, L6

Wertheimer, J. G., & Laughlin, G. 2006, AJ, 132, 1995

West, A. A., Hawley, S. L., Bochanski, J. J., et al. 2008, AJ, 135, 785

Williams, J. G., Sinclair, W. S., & Yoder, C. F. 1978, Geophys. Res. Lett., 5, 943

Williams, J. P., & Cieza, L. A. 2011, ARA&A, 49, 67

Willson, R. C., Gulkis, S., Janssen, M., Hudson, H. S., & Chapman, G. A. 1981, Science, 211, 700

Wood, B. E., Linsky, J. L., Müller, H.-R., & Zank, G. P. 2001, ApJ, 547, L49

Wordsworth, R. D., Forget, F., Selsis, F., et al. 2011, ApJ, 733, L48

Yang, J., Cowan, N. B., & Abbot, D. S. 2013, ApJ, 771, L45

Yoder, C. F. 1995, in Global Earth Physics: A Handbook of Physical Constants, ed. T. J. Ahrens, 1–31

Young, P. A., Desch, S. J., Anbar, A. D., et al. 2014, Astrobiology, 14, 603

Zhang, K., & Hamilton, D. P. 2008, Icarus, 193, 267